

Cosmogenic ^{10}Be and ^{26}Al ages for the Last Glacial Maximum, eastern Baffin Island, Arctic Canada

Kimberly A. Marsella* }
Paul R. Bierman } *Geology Department, University of Vermont, Burlington, Vermont 05405, USA*

P. Thompson Davis *Department of Natural Sciences, Bentley College, Waltham, Massachusetts 02452, USA*

Marc W. Caffee *Center for Accelerator Mass Spectrometry, Lawrence Livermore National Laboratory, Livermore, California 94550, USA*

ABSTRACT

A chronology for the Last Glacial Maximum based on cosmogenic exposure dating in the Pangnirtung Fjord area, eastern Baffin Island, Arctic Canada, is at odds with many decades of land-based, glacial stratigraphic research. Most previous chronologies focused primarily on relative weathering criteria and suggested that ice extent was restricted during the late Wisconsinan (ca. 24–8 ka). In contrast, by directly dating glacial features, we conclude that late Wisconsinan ice was far more extensive than previously believed.

There are 36 gneissic boulders and 8 samples of ice-molded gneissic bedrock that yield late Wisconsinan ^{10}Be and ^{26}Al exposure ages for the last glaciation of Pangnirtung Fjord. The prominent Duval moraines, which were previously interpreted to represent a significant early Wisconsinan (100–60 ka) ice advance on southern Cumberland Peninsula, were actually deposited between 24 and 9 ka. Two boulders from a raised glaciomarine delta, stratigraphically related to the Duval moraines, date to about 10 ka. Two recessional moraines and striated bedrock along Pangnirtung Fjord, as well as erratics on the floor of the Kolik River valley, a tributary to Pangnirtung Fjord, indicate that deglaciation began between 12 and 9 ka.

In situ produced ^{10}Be and ^{26}Al abundances indicate that ice filled Pangnirtung Fjord for about 15 k.y. (either continuously or intermittently) prior to 10 ka, which is compatible with ^{14}C chronologies for adjacent Cumberland Sound. Thus, our data support other recent studies that suggest the northern and southern margins of the Laurentide ice sheet were generally in phase during the latest Wisconsinan, contrary to earlier interpretations.

Keywords: Baffin Island, cosmogenic exposure dating, dating, deglaciation, Laurentide ice sheet, Last Glacial Maximum.

BACKGROUND

The majority of Arctic Canada was ice covered during much of the Quaternary; however, the vertical and lateral extents of ice sheets in the eastern Canadian Arctic have been debated for the past century (Daly, 1902; Cole-

man, 1920; Odell, 1933; Flint, 1943; Løken, 1966; Ives, 1978; Andrews, 1987). Arctic ice-sheet configuration during the late Wisconsinan (ca. 24–8 ka) remains controversial, primarily because glacial landforms were never able to be dated directly until recently. In the past, most of the glacial chronologies were constrained only by relative dating methods and by radiocarbon dating of organic material in marine and lacustrine sediments, not always clearly related to glacial deposits (e.g., Pheasant and Andrews, 1973; Boyer and Pheasant, 1974; Andrews et al., 1975; Birkeland, 1978; Dyke, 1977; Miller et al., 1977; Nelson, 1980). The lack of raised glaciomarine deposits with radiocarbon ages between about 24 and 9 ka suggested minimal isostatic loading, hence restricted ice extent, during the late Wisconsinan (Miller and Dyke, 1974; Andrews, 1975). However, Mayewski et al. (1981) interpreted the same evidence to support extensive ice cover during the late Wisconsinan.

Two different models for the configuration of the northeastern sector of the Laurentide ice sheet during the late Wisconsinan have persisted in the literature since the early 1940s (Ives, 1978). One reconstruction (the minimum ice model), based on interpretation of field data, proposes that ice during the late Wisconsinan glaciation was limited to small, land-based ice caps, leaving the coastal zone of Baffin Island ice free (Miller, 1973; Miller and Dyke, 1974; Andrews, 1975; Dyke and Prest, 1987). In contrast, a second reconstruction (the maximum ice model) supposes that a large, extensive ice sheet with both land- and marine-based domes existed during the late Wisconsinan (Hughes et al., 1977; Denton and Hughes, 1981; Grosswald, 1984).

This paper presents cosmogenic ^{10}Be and ^{26}Al data that pertain to the prominent Duval moraines and related glacial features in the Pangnirtung Fjord area on southern Cumberland Peninsula, Baffin Island (Fig. 1). The Pangnirtung Fjord area (Fig. 1) was investigated for three reasons: (1) the Duval moraines, a major moraine system, are well exposed and purportedly separate two zones with distinguishable degrees of relative weathering; (2) the area lacks adequate numerical dating control; (3) the predominant lithologies are quartz-rich Precambrian gneisses and quartz monzonites, which provide sufficient quartz for ^{10}Be and ^{26}Al in situ-produced cosmogenic isotope dating. The Duval moraines mark the most significant ice advance on southern Cumberland Peninsula; however, the previously estimated early Wisconsinan age (100–60 ka; Dyke, 1977, 1979) is at odds with recent work (Jennings, 1993; Jennings et al., 1996) that shows evidence for late Wisconsinan till on the floor of adjacent Cumberland Sound and onto the southeastern Baffin Island shelf.

*Present address: Department of Geology, Skidmore College, Saratoga Springs, New York 12866, USA; e-mail: kmarsell@skidmore.edu.

FIELD AREA

Physiography

Cumberland Peninsula, southeastern Baffin Island, is underlain primarily by crystalline rock of the Precambrian Canadian Shield, medium- to coarse-grained Archean gneisses, and quartz monzonites (Jackson and Taylor, 1972). Following a period of rifting west of Greenland, tectonic uplift produced the topographic asymmetry of Baffin Island, with the majority of high mountains and deep fjords located along its eastern coast. The landscape of Cumberland Peninsula is dominated by glacial ice, including the Penny ice cap (Fig. 1), as well as hundreds of cirque and valley glaciers. Pangnirtung Fjord, 45 km long and 1 to 3 km wide, opens into northwest-southeast-trending Cumberland Sound (Fig. 1), which is about 240 km long and 80 km wide. The fjord walls rise steeply to the mountains, except at the mouths of large river valleys (e.g., the Kolik River valley; Figs. 1 and 2A). Summit heights increase inland, toward Pangnirtung Pass, a classic, U-shaped valley occupied by the braided Weasel River (Figs. 1 and 2B).

The Pangnirtung Fjord region could have been overrun by ice originating from two major ice sources: the northeastern margin of the Laurentide ice sheet, and/or radial flow from the Penny ice cap. The source of ice in Cumberland Sound during the late Wisconsinan is most likely expansion of the Foxe dome of the Laurentide ice sheet (Fig. 3; Jennings, 1993). Ice at the base of a core from the Penny ice cap (Fig. 1) has $\delta^{18}\text{O}$ values that suggest that the ice was part of a much thicker ice sheet during the Last Glacial Maximum (LGM; Fisher et al., 1998). Thus, ice filling Pangnirtung Fjord, Kingnait Fjord, and the Kolik River valley probably came from a much expanded Penny ice cap (Figs. 1 and 3) that may have been part of the Foxe dome of the Laurentide ice sheet.

Climate

Cumberland Peninsula has a cold, relatively dry maritime climate. The summer (June–September) mean annual temperature for Pangnirtung (13 m above sea level [a.s.l.]) is 5.2 °C; the winter (October–May) mean annual temperature is –16 °C. Gilbert and Church (1983) reported a mean January and February air temperature at Pangnirtung of –27 °C and precipitation through the winter averaging 13–40 mm H₂O per month. Mean annual pre-

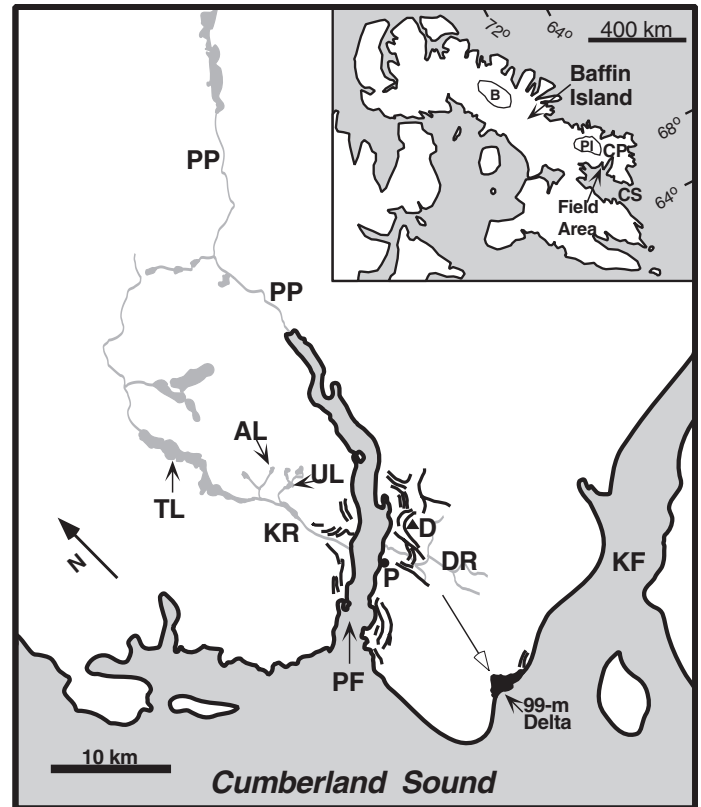


Figure 1. Location map of Baffin Island (inset; B—Barnes ice cap, PI—Penny ice cap, CS—Cumberland Sound) and Pangnirtung Fjord field area on southeastern Cumberland Peninsula, Baffin Island. CP—Cumberland Peninsula, PF—Pangnirtung Fjord, KF—Kingnait Fjord, P—Pangnirtung hamlet, D—Mount Duval, DR—Duval River, KR—Kolik River, TL—Tasikutaaq Lake, AL—Amarok Lake, UL—Ukalik Lake, PP—Pangnirtung Pass. 99 m delta is labeled. Thick black line segments are moraines mapped by Dyke (1977, 1979).



Figure 2. (A) The Kolik River valley and mouth of the Kolik River on the northern side of Pangnirtung Fjord. (B) Looking northeast at the head of Pangnirtung Fjord and the southern end of Pangnirtung Pass, a classic U-shaped valley.

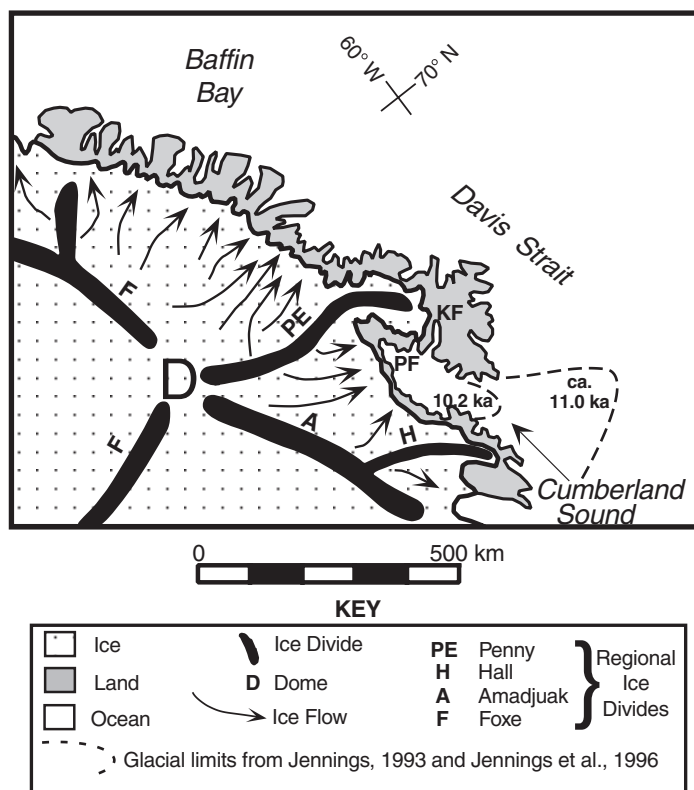


Figure 3. Ice divides for the northeastern margin of the Laurentide ice sheet, Baffin Island (adapted from Dyke and Prest, 1987; 11 ka map). Dashed lines show revised glacial limits from Jennings (1993) and Jennings et al. (1996).

precipitation is about 400 mm, of which 40%–45% falls as rain (Maxwell, 1980). Our field area includes sampling sites as high as 1000 m above sea level (a.s.l.), which probably have greater annual precipitation (perhaps 500 mm), as much as 80% of which is most likely snow (Maxwell, 1980).

Previous Glacial Chronologies in the Eastern Canadian Arctic

The late Wisconsinan ice limit is poorly constrained in the Pangnirtung Fjord area, but was believed to be near the head of Cumberland Sound (Dyke, 1977, 1979). Most existing glacial chronologies for Baffin Island (Fig. 4) suggest that the most extensive glaciation occurred in the early Wisconsinan (ca. 120–60 ka), with ice extending down most fjords. In contrast, the mapped outermost limit of late Wisconsinan ice roughly parallels the fjord heads of the eastern coast of Baffin Island, where the Cockburn moraines have been radiocarbon dated between 8 and 9 ka from shell deposits (e.g., Miller and Dyke, 1974; Andrews, 1975; Dyke, 1977, 1979; Andrews and Ives, 1978; Dyke and Prest, 1987), although Cockburn-age moraines were not identified at the head of Pangnirtung Fjord. The development of glacial chronologies in the eastern Canadian Arctic has relied primarily on morphostratigraphic studies of moraines and shoreline features that have been relatively dated using criteria such as development of felsenmeer and tors (e.g., Boyer and Pheasant, 1974), surface boulder and bedrock weathering (e.g., Dyke, 1977), stages of soil development (e.g., Birkeland, 1978; Bockheim, 1979), degree of hornblende etching (e.g., Locke, 1979), and depth of soil oxidation (e.g., Nelson, 1980).

Weathering Zones

The recognition of three weathering zones along the entire northeastern margin of the Laurentide ice sheet from Newfoundland to the northern Queen Elizabeth Islands led to the prevailing view of restricted Wisconsinan ice extent (Ives, 1978). In the coastal mountains, three altitudinally distinct weathering zones have been defined, from highest (oldest) to lowest (youngest), as weathering zones 1, 2, and 3 (WZ-1, WZ-2, and WZ-3; Fig. 5). The uppermost zone (WZ-1), primarily mountain summits and uplands with tors and block fields, is the most weathered and should have the highest cosmogenic nuclide abundances. The lowermost zone (WZ-3), including valley bottoms and lower fjord walls, is the least weathered (Pheasant and Andrews, 1973; Boyer and Pheasant, 1974) and should have the lowest nuclide abundances. The intermediate zone (WZ-2) is characterized by moderately weathered till, moraines, and bedrock, and presumably, intermediate nuclide abundances.

In general, the weathering-zone concept suggests that altitudinally separated stratigraphic zones can be distinguished based on the amount of subaerial weathering that each has incurred; hence, weathering zones record different lengths of exposure time over which distinct weathering characteristics have formed (Dyke, 1977). The boundaries between these zones are thought to reflect the former margins of fjord glaciers (Boyer and Pheasant, 1974; Fig. 5) and the upper limit of WZ-3 is commonly believed to represent the maximum extent of ice during the Wisconsinan glaciation (Fig. 5; Ives, 1978).

An alternative view of weathering zones is based on differences in basal thermal regime of ice or snow cover (Sugden, 1977; Sugden and Watts, 1977). If cold-based ice persisted on mountain tops while warm-based ice flowed through the fjords and valleys, the morphology of the lowermost weathering zone (WZ-3) would have been shaped by active ice, accounting for the relatively fresh appearance of rocks in this zone. Cold-based ice in the altitudinally highest zone (WZ-1) would have altered the landscape minimally, preserving landscapes predating the last glaciation (Hughes, 1987). The intermediate zone (WZ-2) represents a zone of transitional basal ice conditions, described by Sugden (1977) as a warm-freezing zone, where ice is at the pressure melting point but there is also some regelation. Sugden and Watts (1977) suggested that erratics may be entrained as ice passes from a warm-based regime (as in WZ-3) to a cold-based regime (as in WZ-1). If the thermal regime model for weathering zones is correct and the entire area were deglaciated rapidly, then the highly eroded WZ-3 should have lower nuclide abundances, whereas the area affected by nonerosive, cold-based ice (WZ-1) should have higher nuclide abundances, because nuclides would be inherited from prior periods of exposure. For this model, nuclide concentration in WZ-2 is difficult to predict a priori.

Pangnirtung Fjord Chronologies

The extensive relative-weathering data of Dyke (1977, 1979) suggest that the Duval moraines separate WZ-3 from WZ-2 (Figs. 5 and 6), according to the regional model presented here. However, Dyke discerned the upper weathering zone as zone B (pre-Duval; Dyke, 1979), separated from weathering zone A by the Duval moraines. On Cumberland Peninsula, Dyke (1979) subdivided weathering zone A into five zones, A5–A1, decreasing in altitude and age from the Duval moraines to neoglaciated deposits; in this paper we have used the WZ-1, WZ-2, WZ-3 terminology of the regional model (e.g., Boyer and Pheasant, 1974).

Dyke proposed that the Duval moraines were deposited between 100 and 60 ka based on isostatic evidence and correlation with a stratigraphically related, raised glaciomarine delta (99 m a.s.l. delta; Fig. 1). Because late Wisconsinan ice margins were believed to be well inland of Cumberland Sound, represented by a marine limit of about 55 m a.s.l. at Pangnirtung (~8000

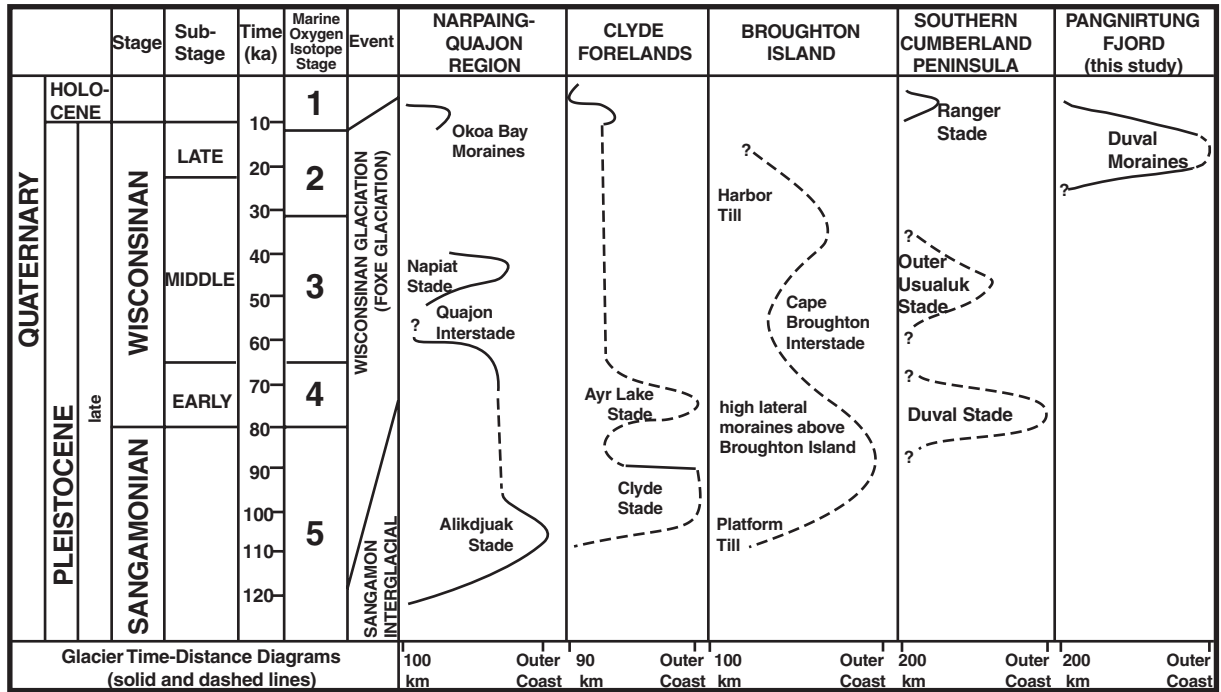


Figure 4. Glacial time-distance diagrams showing the correlation of tills, moraines, and glacial events on eastern Baffin Island (adapted from Nelson, 1980; Pheasant and Andrews, 1973; Miller et al., 1977; Andrews et al., 1975; Dyke, 1977, 1979).

¹⁴C yr B.P.; Dyke, 1977, 1979), Dyke interpreted higher marine limits, such as that represented by the 99 m delta, to be early Wisconsinan in age. In addition, a single amino acid ratio from a reworked shell fragment collected from the delta (Dyke, 1977) was similar to that of shell fragments from the type locality of the Quajon interstade on northern Cumberland Peninsula, which was dated as >29000 ¹⁴C yr B.P., and 59000 ± 18000 yr B.P. by uranium series (Andrews et al., 1975). This 99 m delta sample was the only shell material from the Cumberland Sound area that was interpreted to be pre-Holocene in age (Dyke, 1979) and provided the only numerical age estimate for the Duval moraines.

Since the work of Dyke (1977, 1979), some researchers (e.g., Davis, 1988; Lemmen et al., 1988; Davis et al., 1992; Jennings, 1989, 1993) have hypothesized that late Wisconsinan ice may have been more extensive in the Pangnirtung Fjord area than previously mapped and that the Duval moraines may be late Wisconsinan in age. For example, Lemmen et al. (1988) postulated that ice filled the upper Kolik River valley during late Wisconsinan time, based on bulk organic material dating to 7580 ± 140 ¹⁴C yr B.P. from the base of laminated silts in Tasikutaq Lake (Fig. 1). Thus, ice was at least 60 km more extensive than proposed by Dyke et al. (1982).

Dyke (1977, 1979) and Dyke et al. (1982) also suggested that ice did not extend into Cumberland Sound during at least the past 70 k.y. However, sediment cores from Cumberland Sound (Jennings, 1989, 1993) demonstrate that till, overlain by ice-proximal to ice-distal glaciomarine sediments, was deposited during the late Wisconsinan. The marine sediment record on the continental shelf near the mouth of Cumberland Sound suggests that ice advanced to its maximum position by about 11000 ¹⁴C yr B.P., then retreated up the sound by 10200 ¹⁴C yr B.P. (Jennings et al., 1996; Fig. 3). A black, kaolinite-rich facies in marine sediment cores on the slope off Cumberland Sound has been interpreted to indicate several episodes of glacial erosion during the Wisconsinan glaciation (Aksu and Mudie, 1985; Andrews et al., 1998b). Although the Cumberland Sound ice reconstructions presented in

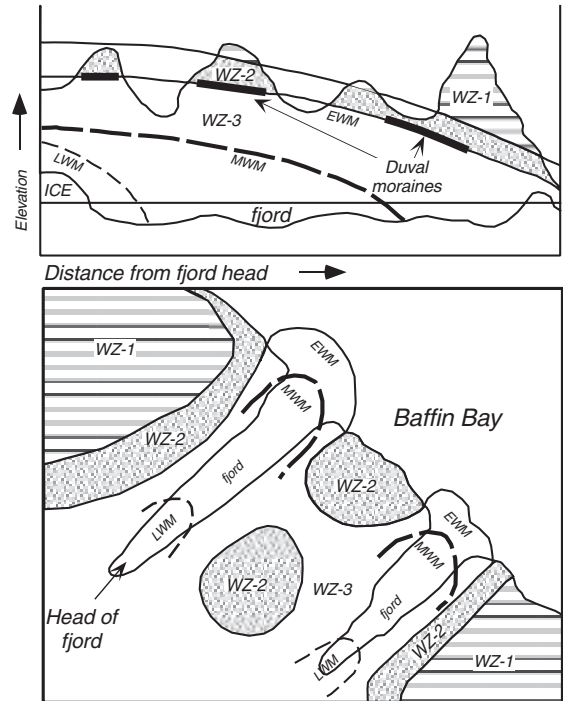


Figure 5. A schematic portrayal of the Quaternary glaciation model for eastern Baffin Island, including Cumberland Peninsula. The upper diagram shows the vertical distribution of lateral moraines and weathering zones on a longitudinal profile. The lower diagram shows the same in planimetric view of highlands dissected by fjords. WZ—weathering zone, EWM—early Wisconsinan moraine, MWM—mid-Wisconsinan moraine, LWM—late Wisconsinan moraine (adapted from Dyke, 1977).

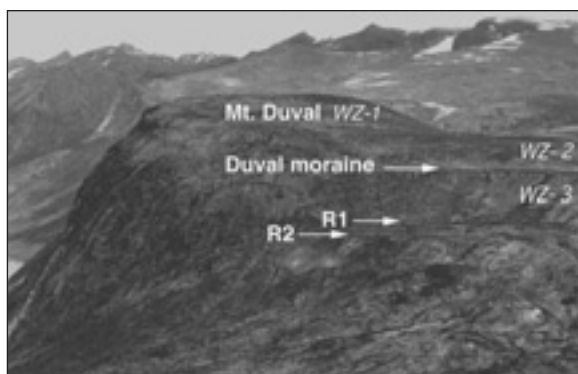


Figure 6. Looking east at type locality of the Duval moraines, separating weathering zones WZ-2 and WZ-3, recessional moraines R1 and R2, and Mount Duval (about 700 m). Foreground field of view is about 1.5 km.

Jennings (1989, 1993) and Jennings et al. (1996) suggest that ice extended well beyond the late Wisconsinan ice margin in Cumberland Sound mapped by Dyke (1977, 1979), this evidence conflicted with the alleged early Wisconsinan age for the most recent glaciation in the Pangnirtung and Kingnait Fjord areas.

The cosmogenic nuclide data presented in this paper, including 12 measurements from Duval moraines, test and confirm the hypothesis that late Wisconsinan ice was far more extensive than originally mapped by Dyke (1977). Thus, the data help to reconcile the discrepancy between the marine and terrestrial records in the Pangnirtung Fjord–Cumberland Sound area and support the notion that the northern and southern margins of the Laurentide ice sheet were generally in phase during the late Wisconsinan.

METHODS

Field Methods

Samples were collected from the Pangnirtung Fjord area during the summer of 1995. Using sledge hammers and chisels, we sampled glacially molded or striated bedrock and the tops of large boulders. All samples are gneiss, quartz monzonite, or quartz veins. Each sample site was located on topographic maps (1:50 000 and 1:250 000 scales) and air photos (1:15 000 and 1:60 000 scales), using a portable global positioning system to obtain latitude and longitude data (± 30 m) and less precise elevation data (± 90 m). Altimeters were used in conjunction with barometric data loggers to obtain more precise elevation data (± 5 – 10 m). The elevation data were adjusted by comparing the logged barometric data with the record of atmospheric pressure from the airport in Pangnirtung, which resulted in corrected elevations accurate to ± 30 m, yielding a $\pm 3\%$ uncertainty when calculating model exposure ages (Appendix A of Marsella, 1998). Geomorphic descriptions of each sample site included the dip, height, length, width, thickness, exposure geometry, and maximum relief of the sampled surface (Appendix B of Marsella, 1998).

Samples were chosen on the basis of three criteria: (1) the likelihood that the site was not covered by till or snow since deglaciation, (2) the likelihood that the sample had not moved since deglaciation, and (3) the likelihood that the sampled surface had not eroded since deglaciation. In most of the field area, till cover is very thin (< 20 cm) and the maximum annual precipitation is < 500 mm, minimizing potential for till and snow cover to affect calcu-

lated model exposure ages. We sampled only the largest and tallest boulders, usually from moraine crests, and far from any slopes to ensure that the samples had neither rolled nor moved into their current orientations. The sampled surfaces varied from unweathered striated bedrock to weathered boulders with maximum crystal relief of 3–4 cm.

Laboratory Methods

Samples were prepared at the University of Vermont following standard methods (Kohl and Nishiizumi, 1992) with some modifications (Marsella, 1998). Samples were crushed, ground, and sieved, retaining the 250–710 μm fraction. Samples were then sonicated at 65°C for 12 h in a solution of 4% HF–4% HNO_3 to remove clays and meteoric ^{10}Be , rinsed, and then sonicated for 12 h in a solution of 6N HCl to remove Fe.

Quartz mineral separates were repeatedly sonicated in a 1% HF–1% HNO_3 solution at 65°C . Sonication produced nearly pure quartz containing < 200 ppm Al, Fe, and Ti (determined by inductively coupled argon plasma spectroscopy [ICP]). Samples containing > 200 ppm of Al, Fe, or Ti were subjected to another cycle of etching in HF– HNO_3 and HCl. All of the samples were then subjected to one final etching in 4% each HF– HNO_3 for 12 to 14 h.

Samples were processed in batches of seven along with a laboratory processing blank of Be and Al carrier. After weighing the quartz (typically 20–40 g), 200–300 μg of commercial Be carrier were added, and the sample was dissolved in 48% HF. No Al carrier was added.

Be and Al fractions were isolated using cation exchange. BeOH and $\text{Al}(\text{OH})_3$ were precipitated with NH_4OH , dried, heated to produce oxides, mixed with pure Ag, and packed into targets for analysis at Lawrence Livermore National Laboratory's (LLNL) Center for Accelerator Mass Spectrometry.

Model Exposure Age Calculations

Measured isotopic ratios were corrected for ratios measured in process blanks by subtracting average ratios for blanks run together on the LLNL accelerator. The $^{26}\text{Al}/\text{Al}$ blanks were low and usually represented only one or two counts; the median $^{26}\text{Al}/\text{Al}$ blank was 3.8×10^{-15} . The $^{10}\text{Be}/\text{Be}$ blanks were higher and less uncertain as they reflect the ^{10}Be content of our carrier solution; the median $^{10}\text{Be}/\text{Be}$ blank for 19 sample batches associated with this project was 3.2×10^{-14} , compared to our long-term laboratory average of $2.4 \times 10^{-15} \pm 9 \times 10^{-16}$. For ^{26}Al , blank subtraction typically represented only 1% of the measured ratio and is thus insignificant in relation to counting statistics-dominated uncertainties for these young samples. For ^{10}Be , the blank correction typically represented 20% of the measured ratio and represents a significant part of the uncertainty of measured ratios and calculated nuclide abundances. Cosmogenic nuclide measurements for recently deglaciated Crater Lake in Pangnirtung Fjord demonstrates that our 2σ detection limits at sea level are 500–1000 yr for ^{26}Al and about 2000 yr for ^{10}Be for this data set (Davis et al., 1999).

Calculated abundances were corrected for sample thickness, latitude, and altitude after Lal (1991) considering only neutrons; no corrections were made for sample geometry because none of the samples collected were from surface edges, none were significantly shielded by horizon geometry, and none dipped more than 40° (a 5% correction). We used the production rates of Nishiizumi et al. (1989) to calculate model exposure ages. However, the production rates of ^{10}Be and ^{26}Al remain uncertain (Clark et al., 1995; Larsen, 1996). If the production rates of Nishiizumi et al. (1989) are overestimated by 10%–20%, our model exposure ages would systematically increase by a similar percentage; however, because our samples are from high latitudes (about 66°N), nuclide production rates are not time dependent (Lal, 1991).

Each sample was analyzed for both ¹⁰Be and ²⁶Al; an average age for each sample was determined using a weighted method, which takes into account the uncertainty associated with each measurement. In general, the Be and Al model exposure ages are well correlated for each sample (Fig. 7; r² = 0.98). In order to facilitate comparison between different sample populations, the uncertainty associated with each exposure age represents the propagation of only laboratory uncertainties, along with a 3% uncertainty in our barometric altitude determinations. When comparing to other chronometers, a 20% uncertainty for nuclide production rates should be considered.

RESULTS AND INTERPRETATIONS

Exposure age data pertinent to the age of the Duval moraines and glacial history of the field area include: (1) the type-Duval region, including boulders on the type-Duval moraine, striated bedrock near the moraine, and recessional moraine boulders (Table 1); (2) Duval-equivalent moraines from both sides of the fjord (Table 2); (3) areas outside of the Duval moraines (Table 3; WZ-1 and WZ-2); (4) the raised 99 m glaciomarine delta on the northern side of Kingnait Fjord (Table 4); and (5) the Kolik tributary valley, including regions inside and outside of the Duval moraine limit (Table 5). The results of the cosmogenic data are presented for each of the five areas noted above, followed by an interpretation of the ages, area by area.

Type-Duval and Duval-Equivalent Moraines

Prominent Duval moraines are extensive along both sides of Pangnirtung Fjord. The type locality of the Duval moraines is located between 470 and 500 m a.s.l. southeast of the hamlet of Pangnirtung. Both the type-Duval moraines and the recessional moraines below them are dissected by large gullies that feed into the Duval River (Fig. 6). The type-Duval moraine is single crested on the upfjord side of the Duval River, but becomes distinctly double crested on the downfjord side (Fig. 8).

Results. Boulder samples on the Duval moraines range in age from 9.2 to 23.4 ka, with one mode in the early part of the late Wisconsinan (21.8 ± 2.2 ka, 1σ, n = 3) and the other mode in the latest Wisconsinan (10.1 ± 1.5, 1σ, n = 3). Two of the three younger ages are from boulders sampled on the inner ridge crest where the type-Duval moraine is double crested (Fig. 8).

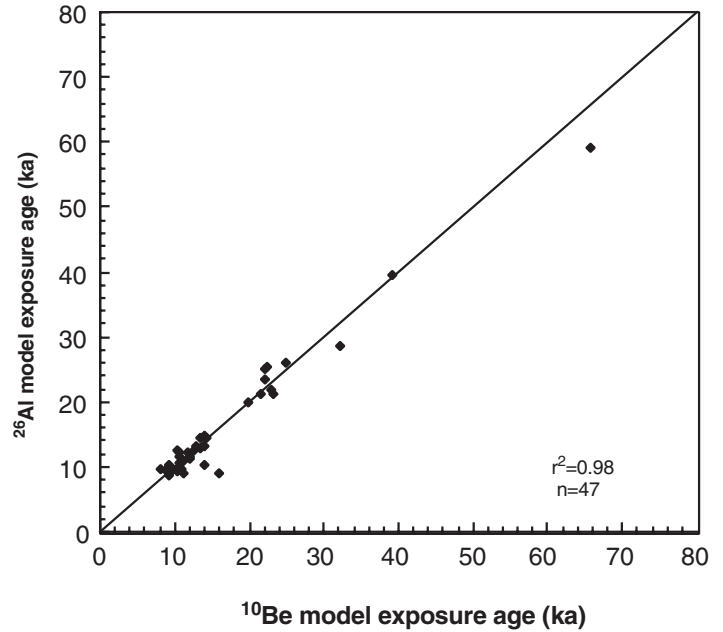


Figure 7. ²⁶Al vs. ¹⁰Be model exposure ages (ka) for all samples reported except sample KM95-16. Solid line represents 1:1 ratio of ²⁶Al and ¹⁰Be model ages.

The older samples occur on the outer crest and the farthest downfjord segment of the type-Duval moraine (Fig. 8). Although the cosmogenic ages yield a range of ages in the late Wisconsinan with two seemingly distinct modes, the samples do not physically appear to be different; all boulders are of the same gneissic lithology, of similar size, and have a similar degree of surface weathering (Fig. 9).

For individual boulders on the type-Duval moraine, the ¹⁰Be and ²⁶Al ages are concordant (Table 1) and a replicate analysis made on sample KM95-35 (Table 1) indicates that our measurements are reproducible. Sam-

TABLE 1. ISOTOPIC DATA FOR THE TYPE DUVAL REGION (LAT 66°8'N, LONG 65°39'W), BAFFIN ISLAND

Sample*	Site†	Sample type‡	Elevation (m)	¹⁰ Be model age (ka)#	²⁶ Al model age (ka)#	Average age** (26Al, 10Be)	²⁶ Al/ ¹⁰ Be	¹⁰ Be measured (10 ⁶ atom g ⁻¹)	²⁶ Al measured (10 ⁶ atom g ⁻¹)
KM95-006	TD	Bldr	500	11.9 ± 0.7	11.7 ± 0.8	11.8 ± 0.7	6.0 ± 0.5	0.11 ± 0.006	0.68 ± 0.04
KM95-007	TD	Bldr	493	9.0 ± 0.7	9.3 ± 0.6	9.2 ± 0.7	6.3 ± 0.6	0.09 ± 0.006	0.54 ± 0.03
KM95-034	TD	Bldr	495	8.9 ± 1.3	9.5 ± 0.6	9.4 ± 1.3	6.5 ± 1.0	0.05 ± 0.007	0.35 ± 0.02
KM95-033	TD	Bldr	495	22.4 ± 1.1	25.3 ± 1.5	23.4 ± 1.1	6.8 ± 0.4	0.22 ± 0.009	1.47 ± 0.07
KM95-035	TD	Bldr	470	N.D.	19.9 ± 1.3	N.D.	N.D.	N.D.	1.13 ± 0.06
KM95-035††	TD	Bldr	470	19.8 ± 1.4	18.2 ± 1.2	18.9 ± 1.4	5.6 ± 0.5	0.18 ± 0.012	1.03 ± 0.06
KM95-036	TD	Bldr	470	22.8 ± 2.6	21.7 ± 1.3	22.0 ± 2.6	5.8 ± 0.7	0.14 ± 0.015	0.79 ± 0.04
KM95-039	DB	Bed	425	22.2 ± 1.1	24.9 ± 1.6	23.1 ± 1.1	6.8 ± 0.5	0.20 ± 0.008	1.34 ± 0.07
KM95-040	DB	Bed	425	24.9 ± 1.3	26.0 ± 1.8	25.3 ± 1.3	6.3 ± 0.5	0.23 ± 0.010	1.44 ± 0.09
KM95-005	R1	Bldr	329	14.3 ± 1.2	14.4 ± 1.0	14.3 ± 1.2	6.1 ± 0.6	0.09 ± 0.007	0.53 ± 0.03
KM95-113	R1	Bldr	271	10.9 ± 1.3	9.5 ± 0.7	9.8 ± 1.3	5.3 ± 0.7	0.08 ± 0.009	0.44 ± 0.03
KM95-114	R1	Bldr	271	11.2 ± 1.5	10.8 ± 0.9	10.9 ± 1.5	5.8 ± 0.9	0.09 ± 0.012	0.51 ± 0.04
KM95-004	R2	Bldr	300	9.5 ± 2.1	9.3 ± 0.9	9.3 ± 2.1	6.0 ± 1.4	0.06 ± 0.012	0.33 ± 0.03
KM95-115	R2	Bldr	266	10.4 ± 1.2	9.4 ± 1.1	9.9 ± 1.2	5.5 ± 0.9	0.08 ± 0.009	0.44 ± 0.05
KM95-116	R2	Bldr	266	9.3 ± 1.3	9.9 ± 0.9	9.7 ± 1.3	6.5 ± 1.0	0.07 ± 0.010	0.47 ± 0.04
KM95-117	R2	Bldr	271	9.3 ± 1.5	9.9 ± 0.9	9.8 ± 1.5	6.5 ± 1.2	0.07 ± 0.011	0.46 ± 0.04

Note: N.D.—not determined.
 *Samples shown in Figure 8.
 †TD—Type Duval; DE—Duval equivalent; DB—Duval bedrock; R1—upper recessional; R2—lower recessional.
 ‡Bldr—boulder, Bed—glacially molded bedrock.
 #Uncertainty represents analytical precision propagated with 3% uncertainty in production rates resulting from barometric altitude determination.
 **Weighted average calculated considering uncertainty of each measurement.
 ††Replicate sample.

TABLE 2. ISOTOPIC DATA FOR DUVAL MORaine EQUIVALENTS, BAFFIN ISLAND

Sample*	Site [†]	Sample type [§]	Elevation (m) ⁶	¹⁰ Be model age (ka) [#]	²⁶ Al model age (ka) [#]	Average age** (²⁶ Al, ¹⁰ Be)	²⁶ Al/ ¹⁰ Be	¹⁰ Be measured (10 ⁶ atom g ⁻¹)	²⁶ Al measured (10 ⁶ atom g ⁻¹)
KM95-009	DE-1	Bldr	665	13.3 ± 0.8	14.6 ± 1.0	13.8 ± 0.8	6.6 ± 0.5	0.15 ± 0.007	0.99 ± 0.06
KM95-024	DE-2	Bldr	455	39.2 ± 1.8	39.5 ± 2.5	39.3 ± 1.8	6.1 ± 0.4	0.36 ± 0.012	2.18 ± 0.12
KM95-025	DE-2	Bldr	445	9.2 ± 0.6	10.2 ± 0.8	9.6 ± 0.6	6.7 ± 0.6	0.08 ± 0.005	0.55 ± 0.04
KM95-028	DE-3	Bldr	375	9.0 ± 0.6	9.4 ± 0.7	9.2 ± 0.6	6.4 ± 0.6	0.08 ± 0.004	0.49 ± 0.03
KM95-029	DE-3	Bldr	380	14.1 ± 0.9	14.8 ± 1.1	14.4 ± 0.9	6.4 ± 0.6	0.12 ± 0.007	0.78 ± 0.05

*Samples shown in Figures 8 and 17.

[†]DE—Duval moraine equivalents; all samples are boulders; DE-1 labeled in Figure 8; DE-2 and DE-3 labeled in Figure 17.

[§]Bldr—boulder.

[#]Uncertainty represents analytical precision propagated with 3% uncertainty in production rates resulting from barometric altitude determination.

**Weighted average calculated considering uncertainty of each measurement.

TABLE 3. ISOTOPIC DATA FOR SAMPLES OUTSIDE THE DUVAL LIMIT, BAFFIN ISLAND

Sample*	Site [†]	Sample type [§]	Elevation [#] (m)	¹⁰ Be model age (ka)**	²⁶ Al model age (ka)**	Average age ^{††} (²⁶ Al, ¹⁰ Be)	²⁶ Al/ ¹⁰ Be	¹⁰ Be measured (10 ⁶ atom g ⁻¹)	²⁶ Al measured (10 ⁶ atom g ⁻¹)
KM95-010	WZ-2	Bldr	728	12.5 ± 0.6	12.4 ± 0.8	12.5 ± 0.6	6.0 ± 0.4	0.15 ± 0.006	0.88 ± 0.05
KM95-011	WZ-2	Bldr	703	9.7 ± 0.6	9.6 ± 0.6	9.7 ± 0.6	6.0 ± 0.5	0.11 ± 0.006	0.68 ± 0.04
KM95-003	WZ-1	Bldr	689	65.8 ± 2.7	59.0 ± 3.6	63.4 ± 2.7	5.7 ± 0.3	0.71 ± 0.021	4.04 ± 0.20
KM95-002	WZ-2	Bldr	657	21.4 ± 1.0	21.2 ± 1.6	21.3 ± 1.0	6.0 ± 0.5	0.23 ± 0.009	1.41 ± 0.09
KM95-101	WZ-2	Bldr	521	23.2 ± 1.3	21.3 ± 1.4	22.3 ± 1.3	5.6 ± 0.4	0.23 ± 0.010	1.26 ± 0.07
KM95-103	WZ-2	Bldr	521	9.2 ± 0.6	8.8 ± 0.7	9.0 ± 0.6	5.8 ± 0.5	0.09 ± 0.006	0.53 ± 0.04
KM95-104	WZ-2	Bldr	521	9.8 ± 0.7	9.5 ± 0.8	9.7 ± 0.7	5.9 ± 0.6	0.10 ± 0.006	0.58 ± 0.05
KM95-100 ^{§§}	WZ-2	Bldr	516	12.1 ± 2.9	11.2 ± 0.8	11.3 ± 2.9	5.6 ± 0.3	0.12 ± 0.015	0.67 ± 0.04
KM95-102	WZ-2	Bldr	501	10.6 ± 0.7	11.7 ± 1.2	10.9 ± 0.7	6.7 ± 0.7	0.10 ± 0.006	0.68 ± 0.06
KM95-105	WZ-2	Bldr	431	9.6 ± 0.7	9.6 ± 0.8	9.6 ± 0.7	6.1 ± 0.6	0.09 ± 0.005	0.52 ± 0.04

*Samples shown in Figure 8.

[†]WZ-2—weathering zone 2; WZ-1—weathering zone 1, mountain summit.

[§]Bldr—boulder.

[#]Samples are presented in altitudinally descending order.

**Uncertainty represents analytical precision propagated with 3% uncertainty in production rates resulting from barometric altitude determination.

^{††}Weighted average calculated considering uncertainty of each measurement.

^{§§}Be and Al measurements from two different aliquots of sample KM95-100.

TABLE 4. ISOTOPIC DATA FOR THE 99-m DELTA, KINGNAIT FJORD (LAT 65°58'N, LONG 65°44'W), BAFFIN ISLAND

Sample*	Site [†]	Sample type [§]	Elevation ⁶ (m)	¹⁰ Be model age (ka) [#]	²⁶ Al model age (ka) [#]	Average age** (²⁶ Al, ¹⁰ Be)	²⁶ Al/ ¹⁰ Be	¹⁰ Be measured (10 ⁶ atom g ⁻¹)	²⁶ Al measured (10 ⁶ atom g ⁻¹)
KM95-138	Adj	Bldr	103	13.9 ± 1.2	10.4 ± 0.8	11.4 ± 1.2	4.6 ± 0.5	0.09 ± 0.007	0.42 ± 0.03
KM95-139	Adj	Bldr	103	9.3 ± 1.8	9.7 ± 1.1	9.6 ± 1.8	6.3 ± 1.4	0.06 ± 0.012	0.39 ± 0.04
KM95-140	Adj	Bed ^{††}	103	10.5 ± 3.1	10.0 ± 0.7	10.0 ± 3.0	5.8 ± 1.7	0.07 ± 0.020	0.40 ± 0.03
KM95-141	Adj	Bed ^{††}	103	10.5 ± 0.7	10.5 ± 0.8	10.5 ± 0.7	6.1 ± 0.6	0.07 ± 0.004	0.43 ± 0.03
KM95-142	On	Bldr	99	9.9 ± 2.6	9.5 ± 1.0	9.6 ± 2.6	5.8 ± 1.6	0.06 ± 0.016	0.37 ± 0.04
KM95-143	On	Bldr	99	13.3 ± 2.3	12.8 ± 1.2	12.9 ± 2.3	5.9 ± 1.1	0.09 ± 0.015	0.50 ± 0.04

*Samples shown in Figure 14.

[†]Adj—samples adjacent to the delta surface, On—samples on delta surface.

[§]Bldr—boulder, Bed—molded bedrock.

[#]Uncertainty represents analytical precision propagated with 3% uncertainty in production rates resulting from barometric altitude determination.

**Weighted average calculated considering uncertainty of each measurement.

^{††}same outcrop.

TABLE 5. ISOTOPIC DATA FOR THE KOLIK RIVER VALLEY REGION (LAT 66°12'N, LONG 65°48'W), BAFFIN ISLAND

Sample*	Site [†]	Sample type [§]	Elevation (m)	¹⁰ Be model age (ka) [#]	²⁶ Al model age (ka) [#]	Average age** (²⁶ Al, ¹⁰ Be)	²⁶ Al/ ¹⁰ Be	¹⁰ Be measured (10 ⁶ atom g ⁻¹)	²⁶ Al measured (10 ⁶ atom g ⁻¹)
KM95-012	KV	Bldr	280	11.8 ± 0.9	12.1 ± 0.9	12.0 ± 0.9	6.2 ± 0.6	0.09 ± 0.007	0.58 ± 0.04
KM95-013	KV	Bldr	280	11.3 ± 1.8	9.0 ± 0.7	9.3 ± 1.8	4.8 ± 0.8	0.09 ± 0.014	0.43 ± 0.03
KM95-014	KV	Bed	280	13.0 ± 1.9	13.2 ± 1.0	13.2 ± 1.9	6.2 ± 1.0	0.10 ± 0.015	0.64 ± 0.04
KM95-015	KV	Bed	280	8.0 ± 1.2	9.5 ± 0.9	9.0 ± 1.2	7.2 ± 1.2	0.06 ± 0.009	0.45 ± 0.04
KM95-030	KE	Bldr	25	16.0 ± 3.7	9.1 ± 1.3	9.9 ± 3.7	3.5 ± 0.9	0.12 ± 0.028	0.42 ± 0.06
KM95-016	AL	Tor	928	128.7 ± 5.5	100.1 ± 5.7	114.9 ± 5.5	4.7 ± 0.2	1.79 ± 0.051	8.34 ± 0.37
KM95-017	AL	Cobble	928	32.3 ± 1.4	28.6 ± 1.8	30.8 ± 1.4	5.4 ± 0.3	0.43 ± 0.014	2.28 ± 0.12
KM95-018	AL	Bldr	723	13.9 ± 0.7	13.2 ± 0.9	13.6 ± 0.7	5.8 ± 0.4	0.17 ± 0.007	0.96 ± 0.06
KM95-019	UL	Bldr	524	22.0 ± 1.0	23.5 ± 1.5	22.5 ± 1.0	6.5 ± 0.4	0.21 ± 0.008	1.38 ± 0.07
KM95-020	UL	Bed	524	10.4 ± 0.6	12.6 ± 0.8	11.2 ± 0.6	7.4 ± 0.6	0.10 ± 0.005	0.76 ± 0.04
KM95-021	UL	Bed	559	10.6 ± 0.7	12.3 ± 0.9	11.2 ± 0.7	7.0 ± 0.6	0.11 ± 0.006	0.75 ± 0.05

*Samples shown in Figure 17.

[†]KV—Kolik valley, AL—Amarok Lake valley, UL—Ukalik Lake valley, KE—Kolik esker.

[§]Bldr—boulder, Bed—glacially molded bedrock, Tor—weathered bedrock, Cobble—fresh erratic.

[#]Uncertainty represents analytical precision propagated with 3% uncertainty in production rates resulting from barometric altitude determination.

**Weighted average calculated considering uncertainty of each measurement.

ples KM95-39 and KM95-40 are from the same glacially molded bedrock adjacent to the type-Duval moraine terminus to the southeast (Fig. 8). Sample KM95-39 is from the surface of the weathered gneissic bedrock and KM95-40 is from a polished, striated quartz vein that stands only 1 to 2 mm above the bedrock surface (Fig. 10). The similarity of the model exposure ages of these samples (Table 1) indicates that our analyses are robust and the lack of surface relief suggests that erosion of the gneiss has been negligible over the late Wisconsinan. The samples from the molded bedrock (KM95-39 and KM95-40) cluster in the older age group of boulders on the type-Duval moraine, with an average age of 24.2 ka.

Five boulders sampled from three separate Duval-equivalent moraine segments on both sides of Pangnirtung Fjord exhibit a similar age distribution to the younger mode on the type-Duval moraine (Table 2); four of the five exposure ages are between 14.4 and 9.2 ka, and one older outlier age is 39.3 ka. On the basis of the age distribution of boulders on all Duval moraines sampled, 10 of 11 samples are within the late Wisconsinan age range, specifically between 24 and 9 ka. Only one sample is older than 24 ka (KM95-24; 39.3 ± 1.8 ka), suggesting that this sample may have inherited some nuclides from a prior period of near-surface exposure.

Interpretation. The Duval moraines represent a significant advance of ice on southern Cumberland Peninsula; thus, the age of these features has important glaciological and climatic significance. Although mapped as early Wisconsinan features (Dyke et al., 1982), our surface exposure dating demonstrates that these features were deposited during the late Wisconsinan. On the Duval moraine, ^{10}Be and ^{26}Al ages are concordant for individual boulders (Table 1). However, the bimodal age distribution of our samples makes interpretation of ice cover complex and nonunique.

Replicate samples and analyses suggest that the age distribution of boulders on the Duval moraines is real and reflects geomorphic processes. We consider three alternatives to explain the range of cosmogenic ages: (1) the age distribution represents erosion of the moraine surface that has removed older boulders, exposing boulders that were previously below the surface (Hallet and Putkonen, 1994); (2) the boulders with lower exposure ages have a history of snow, ice, or till cover (Brook et al., 1993); or (3) the age distribution represents the time period over which boulders were delivered to the moraine (Gosse et al., 1995). We reject alternative 1 because it is based on a model that is applicable to old (>100 ka) moraines. Although the moraines used in the Hallet and Putkonen (1994) study were from the warm, dry eastern side of the Sierra Nevada, we do not expect that moraine

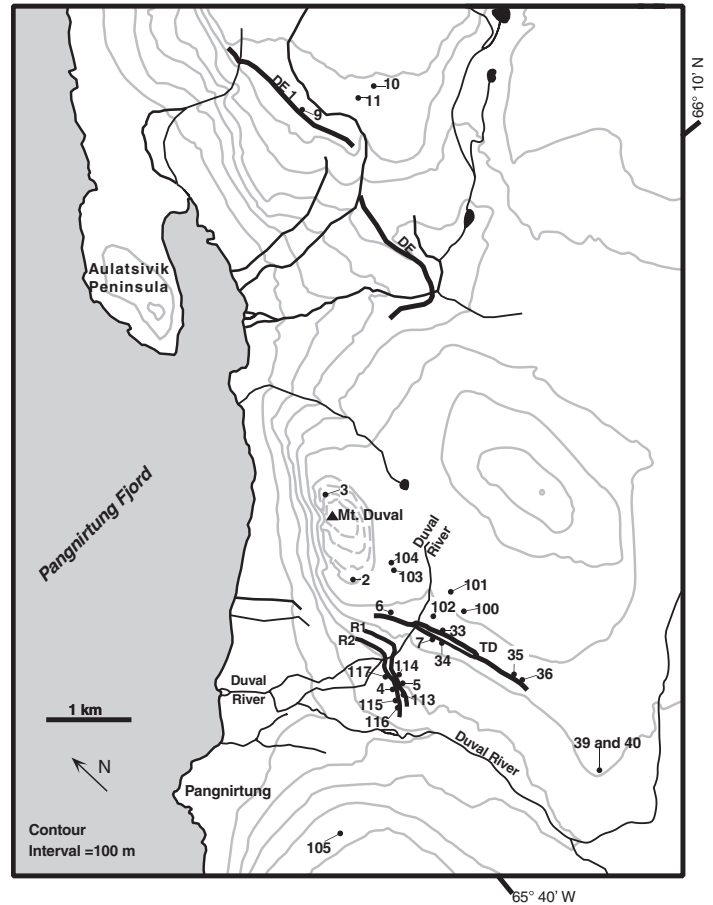


Figure 8. Sample site map for the type-Duval (TD) moraine, Duval recessionals (R1, R2), bedrock samples, and some WZ-2 samples. Numbers represent KM95 sample locations; data are summarized in Table 1. DE—Duval moraine equivalents. Gray solid lines are 100 m contours. Not all moraines mapped by Dyke (as shown in Fig. 1) are represented here; only the most prominent moraines and those mapped in the field in 1995 are shown. Base map derived from part of Canadian Department of Energy, Mines and Resources, 1980, Pangnirtung 26-I/4, 1:50 000 map.



Figure 9. Two gneissic boulder samples from the type-Duval moraine. (A) Sample KM95-33 from the outer crest of the moraine; average exposure age is 23.4 ka (1.75 m person for scale). (B) Sample KM95-34 from the inner crest of the moraine; average exposure age is 9.4 ka (1.7 m person for scale). Spatial relationship of these two boulders, which are of similar size, surface weathering, and lithology, is shown in Figure 8.

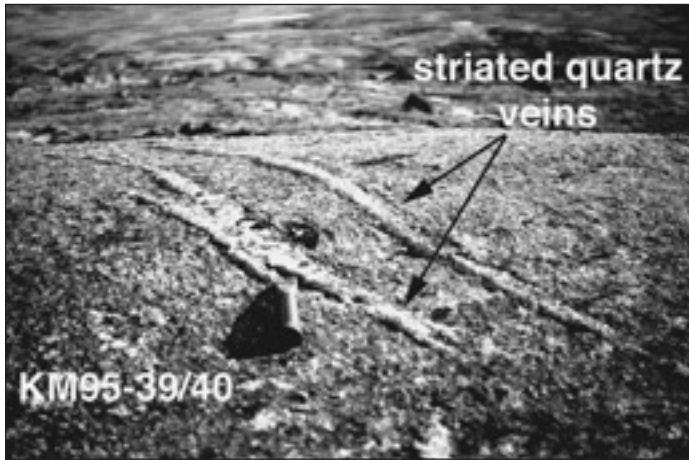


Figure 10. Striated quartz veins (KM95-40) in glacially molded bedrock outcrop (KM95-39) southwest of the type-Duval moraine; weathered bedrock surface is 1–3 mm lower than quartz veins; chisel is 15 cm long.

degradation in our field area, a polar desert, occurs an order of magnitude faster. Furthermore, there is no reason why moraine erosion would yield a distinctly bimodal age distribution. Alternative 2 requires that younger boulders had a different history of snow, ice, or till cover, or surface erosion than older boulders. This scenario is unlikely, because all of the boulders are the same lithology, same size, and located on the same moraines.

We favor alternative 3, which suggests that ice filled Pangnirtung Fjord (either continuously or episodically) to the height of the Duval moraines from about 24 ka (the oldest average age on the moraine) until about 9 ka (the youngest average age on the moraine), implying that the moraine formed over a period of at least 15 k.y. Because we cannot be sure that we sampled both the earliest and the most recently deposited boulders on the moraine, the age range represents a minimum limit; however, the end of deposition on the Duval moraines at 10–9 ka is constrained by the oldest recessional moraine and the stratigraphically related glaciomarine delta, which are discussed later. The geomorphic distribution of the boulders on the type-Duval moraine (Fig. 8) suggests that the initial advance may have been slightly more extensive than later advances, as represented by outer and inner moraine crests, respectively. Thus, our data indicate that either the ice margin fluctuated near the Duval moraines during the late Wisconsinan, from about 24 to 9 ka, or ice retreated around 24 ka and readvanced about 10 to 9 ka. In either case, it is clear that the Duval moraines are much younger than previously thought.

Duval Recessional Moraines

Although the type-Duval moraine and its equivalents are recognizable and extensive along both sides of Pangnirtung Fjord, prominent recessional moraines were observed only below the type-Duval moraines. The two most distinct, nested recessional moraines were sampled (Figs. 6 and 8). Recessional moraine R1 is about 600 m west and 200 m downslope of the type-Duval moraine. Recessional moraine R2 is 150 m farther west and 10–30 m downslope of R1. These moraines are more distinctive on the downfjord side of the Duval River and both are double crested, similar to the type-Duval moraine.

Results. The average exposure ages of both recessional moraines (Table 1) are indistinguishable within one standard deviation from the younger mode of type-Duval moraine ages. The mean age for R2 ($9.5 \pm$



Figure 11. Gneissic boulder samples on R1 (1.75 m person for scale); data are summarized in Table 1. Spatial relationship of these three boulders, which are of similar size, surface weathering, and lithology, are shown in Figure 8.

0.5 ka, 1σ , $n = 4$) is younger than the mean age for R1 (11.9 ± 2.0 ka, 1σ , $n = 3$; Fig. 11), consistent with their stratigraphic relationship. However, the mean age of R1 (11.9 ka) is older than the younger mode of the type-Duval moraine (10.1 ka), and all of the ages from R1 and R2 appear to overlap with the youngest ages on the type-Duval and equivalent moraines. None of these three sample populations can be separated at 95% confidence.

Interpretation. The uncertainty associated with the mean age for all samples on both recessional moraines, 10.5 ± 1.8 ka (1σ , $n = 7$), approaches the resolution of both ^{10}Be and ^{26}Al for dating a single deposit, as most of the single-isotope model exposure ages have an analytical uncertainty of 0.7–2.6 k.y. (Table 1) during the late Wisconsinan. The average ages of the four boulder samples from R2 are tightly clustered; in contrast, the three boulder samples from R1 show a wider scatter of average ages, the age of the youngest boulder on R1 resembling the average exposure age of R2 (Table 1). Thus, the average exposure age of R1 could be an overestimate. Boulders on R1 and R2 may retain some prior exposure history or the younger recessional moraines contain boulders that are intermixed with boulders from earlier glacial events (e.g., Brown et al., 1991). The exposure age chronology for the recessional moraines suggests that they were deposited within at most 2 k.y. after initial retreat from the type-Duval position. Thus, the concordant cosmogenic nuclide data for the Duval moraines and recessional moraines indicate that ice filled Pangnirtung Fjord during the late Wisconsinan and retreated about 10 ka.

Weathered Areas Outside the Duval Moraine Limit

The area directly outside the Duval moraines is an upland plateau region, described by Dyke (1977, 1979) as the pre-Duval terrain, which fits the regional model of the intermediate weathering zone (WZ-2). The area is between the well-defined Duval moraines and the mountain tops (WZ-1; Figs. 5 and 6) and is characterized by felsenmeer. We sampled boulders from WZ-2 as well as from the high tors and mountain tops (WZ-1; Bierman et al., 1999).

There are no distinct ice-marginal landforms located at the break between WZ-2 and WZ-1 (Fig. 6); however, the boulders and bedrock in WZ-1 appear much more weathered than those in WZ-2. In contrast, while Duval-age moraines have been identified regionally as the break between WZ-3 and WZ-2 (Dyke, 1977, 1979; Fig. 6), in our field area we observed that the

boulders in WZ-2 do not appear to be significantly more weathered than those on the Duval moraines. Soil data (Birkeland, 1978; Bockheim, 1979) also discriminate better WZ-2 from WZ-1 than WZ-3 from WZ-2.

Results. Exposure ages for boulders from WZ-2 are similar to exposure ages from the Duval moraines. Samples KM95-100 through KM95-104 (Figs. 8 and 12), from the broad region outside the type-Duval moraine limit, yield exposure ages ranging from 22.3 to 9.0 ka (Table 3). Samples KM95-10 (728 m a.s.l.) and KM95-11 (703 m a.s.l.) are from the broad, upland plateau outside the Duval-equivalent moraines above Aulatsvik Peninsula, about 5 km northeast of Mount Duval (Fig. 8). The exposure ages of these samples range from 12.5 to 9.7 ka (Table 3). In contrast, the samples from WZ-1, including one boulder from the summit of Mount Duval, high tors from above the hamlet of Pangnirtung (Bierman et al., 1999), and the high tors in the Kolik River valley region (discussed later), have much longer and more complex exposure histories. For example, sample KM95-3 (689 m a.s.l.), from the summit of Mount Duval, has model ^{10}Be and ^{26}Al ages of 65.8 ± 2.7 and 59.0 ± 3.6 ka (Table 3).

Interpretation. The weathered areas outside the Duval moraine limit (WZ-2) present a glacial geologic conundrum. Based on the weathering-zone concept (Dyke, 1977, 1979), as well as stratigraphic relationships, samples from these areas were expected to yield exposure ages greater than those collected from the Duval moraines. However, our cosmogenic nuclide data suggest that areas directly outside of the Duval moraines (WZ-2) were not exposed during the late Wisconsinan because exposure ages are ≤ 22 ka. Conversely, the early Wisconsinan age (>59 ka) of sample KM95-3 (Fig. 9; Table 3) suggests that the higher and more distal summit of Mount Duval was either a nunatak, or was covered by cold-based, nonerosive ice during the late Wisconsinan, thus preserving a prior exposure history.

None of the samples from the weathered areas of felsenmeer (WZ-2), just outside the Duval moraine limit, shows evidence for long-term burial (i.e., significant discordance between the ^{10}Be and ^{26}Al ages resulting from $^{26}\text{Al}/^{10}\text{Be} \ll 6.0$; Table 3). All of the exposure ages in WZ-2 are concordant with the distribution of ages on the Duval moraines, suggesting that the Duval moraines do not mark the limit of late Wisconsinan ice in the area, but may instead represent a major stillstand or readvance during the Last Glacial Maximum (LGM). Most important, the cosmogenic nuclide data indicate that the Duval moraines do not mark a chronologically important morphological boundary.

One explanation for the apparent congruence of the weathering-zone boundary and the Duval moraine limit (Dyke, 1977, 1979) is the model of Sugden (1977) and Sugden and Watts (1977), which suggests that altitudi-

nal zones of increased weathering reflect differing glacial thermal regimes. The presence of warm-based ice in fjords and cold-based ice on the highlands between fjords may leave the intermediate upland plateaus as transitional ice zones, similar to situations described by Sugden and Watts (1977) for the eastern coast of Baffin Island. Our exposure age data fit this model, because the nuclide abundances from the uppermost weathering zone (WZ-1) could suggest the presence of cold-based ice (Bierman et al., 1999), whereas the exposure ages for the Duval moraines and striated bedrock outcrops coincident with the Duval moraines (WZ-3) could indicate the presence of warm-based ice in Pangnirtung Fjord. The model of Sugden and Watts (1977) explains the morphology of the intermediate weathering zone (WZ-2) as a zone of transitional basal ice conditions, where erratics may be incorporated into the cold-based ice during transition from a warm-based regime to a cold-based regime, but fails to explain the bimodal age distribution of our samples. Moreover, the glacial thermal regime model is incompatible with the presence of such dramatic morphological features such as the Duval moraines.

Neither the weathering-zone model nor the thermal-regime model clearly explains the age distribution of erratics on the upland plateau just outside of the Duval moraine limit (WZ-2). Specifically, we are unable to explain how most boulders outside the Duval moraines have exposure ages younger than three of the boulders on the moraine. Thus, samples collected just outside the Duval moraine limit suggest that the glacial dynamics and/or isotope systematics are complex. It is possible that the older boulders on and outside the Duval moraines deposited by an earlier 25 ka advance were reworked by an advance at about 10 ka. We can say with confidence that WZ-2 erratics are on average no older than the Duval moraine boulders, and thereby support an expanded ice sheet extent in the Pangnirtung Fjord area during the late Wisconsinan.

Raised 99 m Glaciomarine Delta

The glacial chronology for southern Cumberland Peninsula proposed by Dyke (1977, 1979) depends in part on the ages of raised glaciomarine deltas. The top of one large, raised glaciomarine delta (Fig. 13), located on the northern side of Kingnait Fjord (Figs. 1 and 14), is 99 m a.s.l. The sediment composing this delta was carried through a large meltwater channel (8 km long and to 50 m deep) and a series of smaller meltwater channels that grade proximally to the type-Duval moraines along Pangnirtung Fjord (Fig. 14; Dyke, 1977). This stratigraphic relationship indicates that the delta

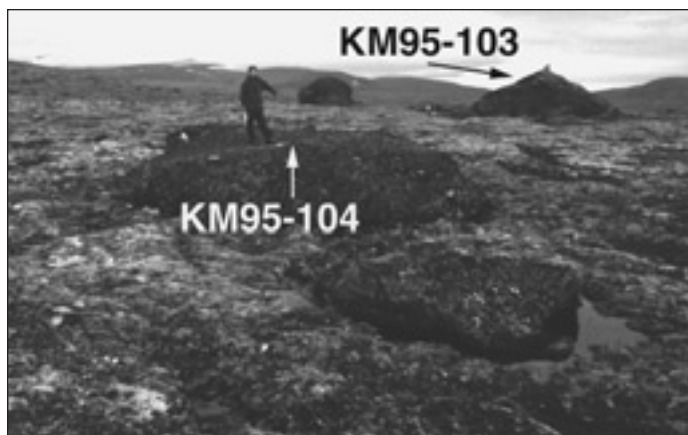


Figure 12. Samples KM95-103 and KM95-104, gneissic boulders from the weathered upland surface outside the Duval moraine limit (1.75 m person for scale); data are summarized in Table 3.

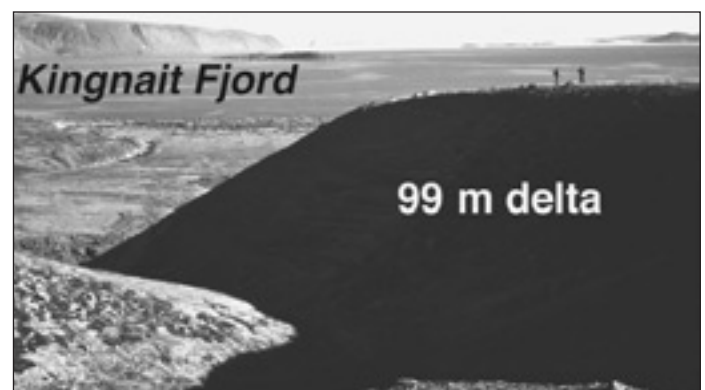


Figure 13. Looking south toward Cumberland Sound across the raised 99 m above sea level glaciomarine delta along outer Kingnait Fjord; two 1.8 m people can be seen on the top surface of the delta.

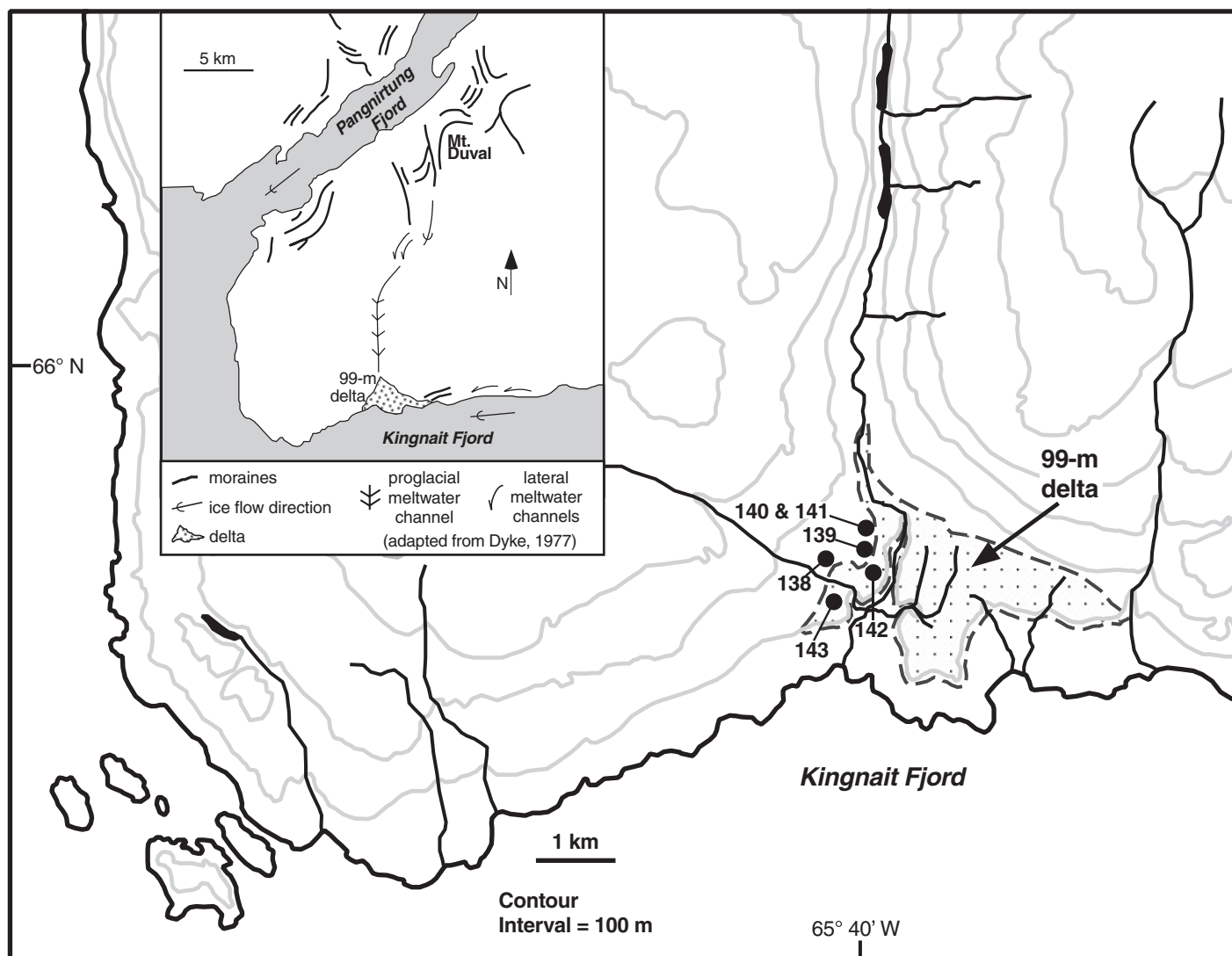


Figure 14. Map showing relationship of the type-Duval moraines to the raised 99 m glaciomarine delta along outer Kingnait Fjord (inset; adapted from Dyke, 1979) and sample site map for the delta. Numbers represent KM95 sample locations; data are summarized in Table 4. Delta surface is represented by stippled pattern. Thick gray solid lines are 100 m contours. Base map is derived from parts of Canadian Department of Energy, Mines and Resources, 1980, Pangnirtung 26-I/4, and Kekertukdjuak Island 26 H/13, 1:50 000 maps.

formed as ice stood at the type-Duval moraines. Two lateral moraine segments along Kingnait Fjord that slope down to the marine limit appear to be overlain by the delta (Fig. 14; Dyke, 1977), indicating that ice retreated from Kingnait Fjord prior to formation of the delta. On the basis of cosmogenic nuclide exposure ages from islands near the mouth of Kingnait Fjord (Davis et al., 1996; Appendix B of Marsella, 1998), these lateral moraine segments are roughly equivalent in age to the Duval moraines. Stratigraphically, the moraines are older than the delta.

Results. We collected six samples on and adjacent to the 99 m delta (Fig. 14; Table 4); four samples come from a few meters beyond the delta surface on the western side, two from large boulders and two from polished bedrock, and two samples are from large boulders on the surface of the delta (Fig. 14). Of these six samples, the two boulders on the delta surface probably provide the closest minimum-limiting age for the delta, and, by association, the Duval moraines, assuming no isotopic inheritance. The mean exposure age of the four samples adjacent to the delta provide a minimum-

limiting age for deglaciation of Kingnait Fjord, and thus provide an estimate for a maximum-limiting age for the delta. The average exposure age of 10.4 ± 0.8 ka (1σ , $n = 4$) for the four samples beyond the delta (Figs. 15 and 16) is similar to the average age of 11.2 ± 2.3 ka (1σ , $n = 2$) for the two boulders on the delta.

Interpretation. Ice withdrew from the Kingnait Fjord area between 11 and 10.5 ka and ice stood at the Duval position (the source of meltwater to form the delta) in Pangnirtung Fjord until about 10.1 ± 1.5 ka (average of young mode from Table 1); thus, the delta must have formed between about 11 and 10 ka. Of the two boulders on the delta surface (KM95-142 and KM95-143), KM95-142 has concordant Be and Al exposure ages (9.9 ± 2.6 and 9.5 ± 1.0 ka) consistent with the interpretation herein. Sample KM95-143 also has concordant Be and Al exposure ages (13.3 ± 2.3 and 12.8 ± 1.2 ka); these ages are older than other exposure ages that constrain final ice retreat from the Duval moraines and from Kingnait Fjord. Sample KM95-143 probably carried with it some inheritance when the boulder was deposited on the delta.

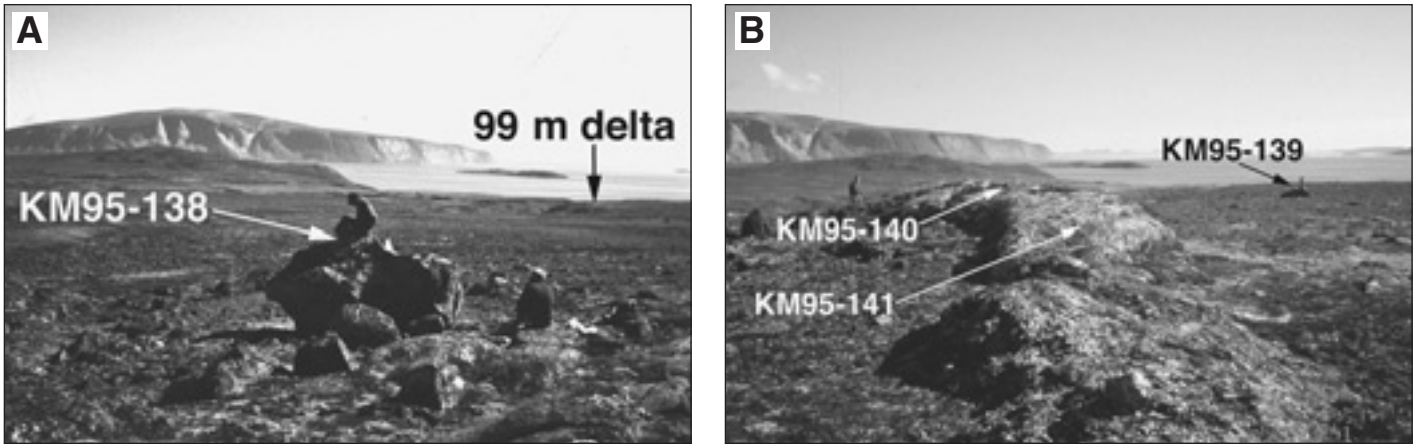


Figure 15. (A) Sample KM95-138 (1.8 m person for scale) and (B) samples KM95-139 to KM95-141 from beyond the raised 99 m delta surface along outer Kingnait Fjord (1.8 m person for scale); data are summarized in Table 4.

The age of the delta is well constrained between about 11 and 10 ka. The delta must be younger than other boulder and bedrock samples in Kingnait Fjord and must be older than samples related to the retreat of ice from the Duval moraines in Pangnirtung Fjord. Conversely, exposure ages from the raised 99 m glaciomarine delta provide additional age constraint for deposition of the Duval moraines during the late Wisconsinan; ice must have remained at the Duval moraines until at least 10 ka to supply meltwater to the delta. If the relative sea-level curve for the Pangnirtung Fjord area determined by Dyke (1979; Fig. 16) is projected upward to include the elevation of the 99 m delta, the delta's age based on the uplift curves would be about 9300 ¹⁴C yr B.P. (Fig. 16), or about 10.2 ka using CALIB 3.0 (Stuiver and Reimer, 1993). Thus, the 11–10 ka age that we propose for the 9 m delta is consistent with the lower marine limits in the area, as well as our independent exposure-age determinations for the Duval moraines.

Kolik River Valley

The braided Kolik River flows through a U-shaped valley (Fig. 2A) and is fed by meltwater from cirque glaciers and outlet glaciers of the Penny ice cap. The Kolik River valley is oriented roughly north-south and drains into Pangnirtung Fjord (Fig. 1). Dyke et al. (1982) suggested that the Kolik River valley was ice free during the late Wisconsinan.

In the Kolik River valley, we identified an esker that grades into ice-contact deltas 4–5 km upstream of the river mouth (Figs. 17 and 18). The esker, a steep-sided, 6-km-long, anastomosing, sinuous ridge composed of well-sorted silt, sand, and gravel, is clearly identifiable on aerial photographs and in the field. Four samples from boulders and bedrock were collected from the valley bottom (KM95-12, KM95-13, KM95-14, and KM95-15; Fig. 19) and one boulder was sampled from the surface of the esker (KM95-30).

Earlier work in the upper Kolik River valley suggested the presence of late Wisconsinan ice (Lemmen et al., 1988; Marsella et al., 1995) upvalley. Although Lemmen et al. (1988) did not suggest that ice completely filled the Kolik River valley during the late Wisconsinan, bedrock samples collected in 1994 adjacent to Tasikutaaq Lake yielded concordant ²⁶Al and ¹⁰Be ages of 12.0 ± 2.7 and 12.3 ± 2.9 ka (Marsella et al., 1995), supporting the hypothesis of Lemmen et al. (1988) that late Wisconsinan ice extended farther down the Kolik River valley than proposed by Dyke et al. (1982).

Results. For logistical reasons, in this study we focused on the lower Kolik River valley, downstream of Tasikutaaq Lake (Figs. 1 and 17). Two sam-

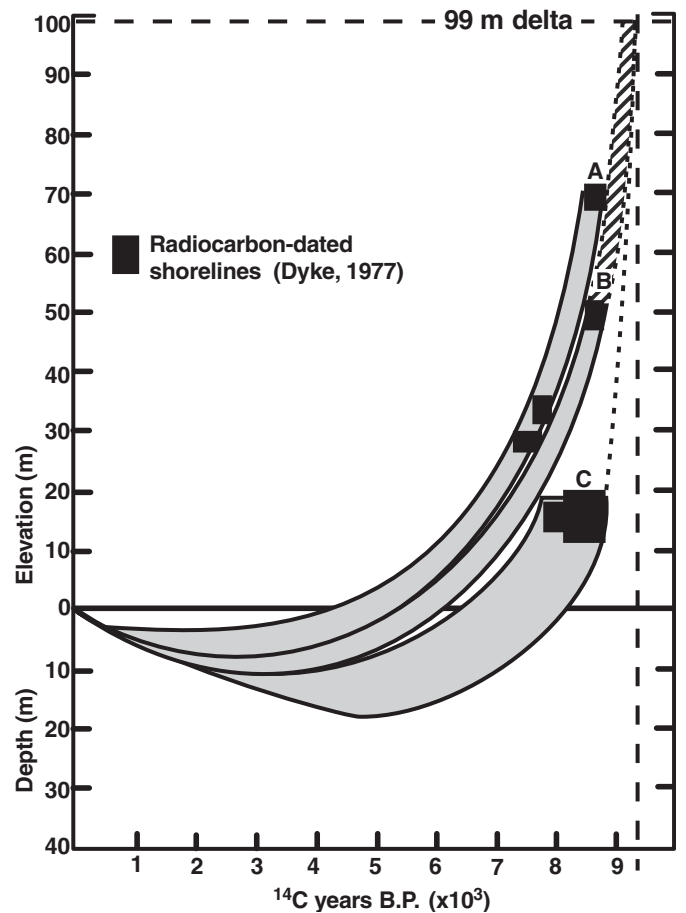


Figure 16. Relative sea-level curves (light shading) and radiocarbon ages (black shading) for Cumberland Sound: A—Usualuk Fjord, B—Pangnirtung Fjord, C—head of Kingnait Fjord (modified from Dyke, 1979). Dashed lines bracketing horizontal bars are the hypothetical extension of the Pangnirtung curve to the height of the raised 99 m delta; dashed vertical line indicates the intersection of this surface with the time axis at about 9300 ¹⁴C yr B.P.

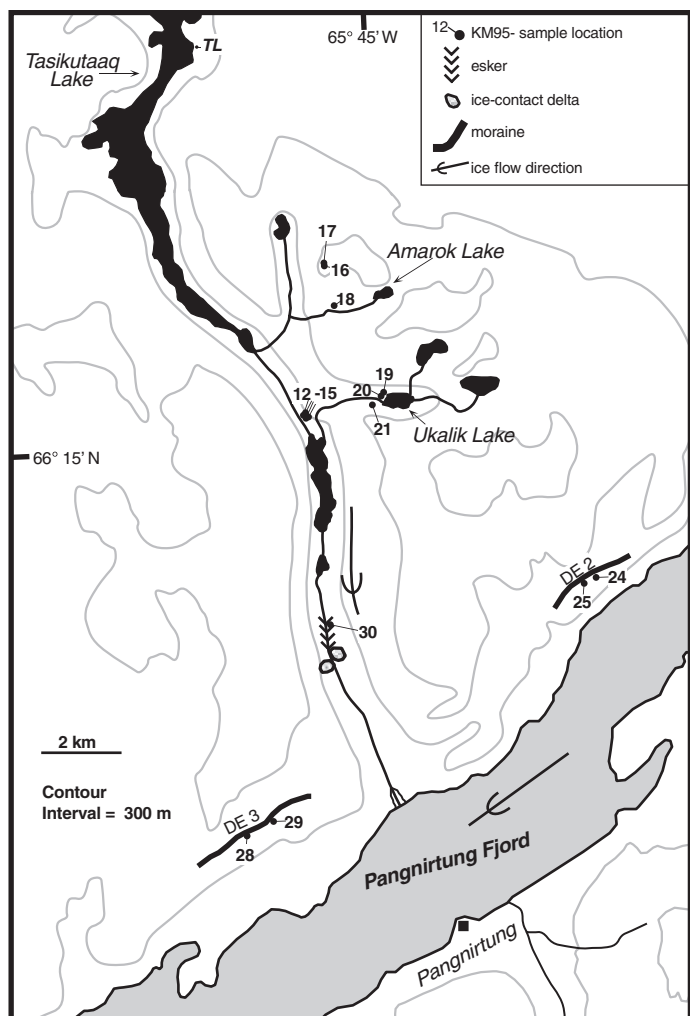


Figure 17. Map showing Kolik River valley sample sites: TL indicates location of cosmogenic age reported by Marsella et al. (1995). Numbers indicate KM95 sample locations; data are summarized in Table 5. Thick solid lines are Duval equivalent (DE) moraines. Thin solid lines are 300 m contours. Base map is derived from part of Natural Resources Canada, 1995, Pangnirtung 26-I, 1:250 000 map.

ples were collected from glacially molded bedrock (KM95-14 and KM95-15) and two samples were collected from large boulders on the bedrock exposures (KM95-12 and KM95-13; Table 5). These samples have a mean age of 11.0 ka (11.0 ± 1.9 ; 1σ ; $n = 4$). The esker-delta complex downstream (Fig. 17) of these four samples must have also formed around this time; however, only one low-lying boulder on the esker (KM95-30) was available for sampling and yielded ^{10}Be and ^{26}Al model exposure ages of 16.0 ± 3.7 and 9.1 ± 1.3 ka, respectively (Table 5).

Interpretation. Exposure age data from the Kolik River valley provide further information for delimiting the timing and extent of glaciation in the field area. Dyke (1977, 1979) recognized that the ice-contact deltas in the Kolik River valley could only have been formed when proglacial lakes were dammed by ice filling Pangnirtung Fjord (Fig. 17). Our data provide the first direct age estimates for landforms in the Kolik River valley and suggest that this tributary valley was filled with ice until about 11 ka, about the same time we suggest that ice began to retreat from Pangnirtung Fjord.

The mean age of 11.0 ± 1.9 ka for samples from the floor of the Kolik River valley (KM95-12 to KM95-15) is indistinguishable from the age of the 99 m delta ($11-10.5$ ka) in outer Kingnait Fjord and the younger Duval moraine ages in Pangnirtung Fjord (10.1 ± 1.5 ka), indicating that the Kolik River valley was filled with ice during the late Wisconsinan and became deglaciated about 11 ka. The ^{26}Al age for KM95-30, the low-lying boulder on the esker, supports this assertion. Based on the 11.0 ka age for deglaciation of the lower Kolik River valley and the relationship of the esker and/or delta system to lakes impounded by ice in Pangnirtung Fjord, we infer that deglaciation of the Kolik River valley began just prior to deglaciation of Pangnirtung Fjord.

Amarok and Ukalik Lake Valleys

The upland regions around the Kolik River valley are characterized by bedrock tors surrounded by a grus-covered felsenmeer surface, yet a record of prior glaciation is preserved here. Although large bedrock tors exhibit weathering features such as micropitting and macropitting and surface disaggregation, fresh erratic cobbles were found on tors in juxtaposition to the felsenmeer and grus surrounding the erosional landforms. At elevations similar to those where tors are found (to 1000 m a.s.l.), molded bedrock forms covered by perched boulders are also common, providing further evidence for previous glacial cover.

Results. The highest-elevation samples collected in the Kolik River valley area are KM95-16, from a bedrock tor, and KM95-17, a fresh erratic cobble (both 928 m a.s.l.) located above the Amarok Lake valley. Sample KM95-16 has minimum-limiting ^{10}Be and ^{26}Al ages of 128.7 ± 5.5 and 100.1 ± 5.7 ka. Sample KM95-17 yields ^{10}Be and ^{26}Al limiting model exposure ages of 32.3 ± 1.4 and 28.6 ± 1.8 ka (Table 5). A single large boulder, sample KM95-18, from the Amarok Lake valley floor has concordant ^{10}Be and ^{26}Al ages of 13.9 ± 0.7 and 13.2 ± 0.9 ka.

Ukalik Lake, south of Amarok Lake, is in a steeply sloping basin 5 km downvalley from a cirque (Figs. 17 and 20). We collected three samples from the bedrock cirque lip of Ukalik Lake; one boulder, KM95-19, and two bedrock samples, KM95-20 and KM95-21 (Fig. 17). Samples KM95-19 and KM95-20 are from the same surface (Fig. 20); the boulder is a fresh erratic and the bedrock is striated and polished. Sample KM95-21 is from one of the many stoss-lee bedrock surfaces observed about 5 m above lake level. The average ^{10}Be and ^{26}Al age of the boulder, sample KM95-19, is 22.5 ± 1.0 ka, whereas both bedrock surfaces have average exposure ages of 11.2 ± 0.7 ka (Table 5).

Interpretation. Our cosmogenic exposure age data suggest that the Ukalik and Amarok Lake were deglaciated during the late Wisconsinan. Model exposure ages of the high bedrock tor above Amarok Lake (KM95-16) are >100 ka; the measured $^{26}\text{Al}/^{10}\text{Be}$ ratio of 4.7 ± 0.2 (Table 5) suggests that this sample has a long and complex burial and exposure history, similar to six other samples from the high plateau area south of Pangnirtung Fjord (Bierman et al., 1999). Thus, nuclide abundances from KM95-16 cannot be interpreted as simple exposure ages. The age of the cobble (KM95-17) sitting on the tor provides more insight into the glacial history. If KM95-17 is a tillstone, model exposure ages of 32.3 ± 1.4 and 28.6 ± 1.8 ka for ^{10}Be and ^{26}Al (Table 5) suggest that cold-based ice covered the tor until about 30 ka. This exposure age is uncertain, as the measured $^{26}\text{Al}/^{10}\text{Be}$ ratio for KM95-17 is 5.4 ± 0.3 , suggesting that the cobble may have been buried or shielded from cosmic rays during or after exposure. It is also possible that the cobble carries nuclides from a prior period of exposure.

The single large boulder, KM95-18, sampled from the Amarok Lake valley floor has concordant ^{10}Be and ^{26}Al ages, consistent with ice retreat from the Amarok Lake valley before 13.6 ka. If the 13.6 ka age is representative of the entire Amarok Lake valley floor, this exposure age suggests that an

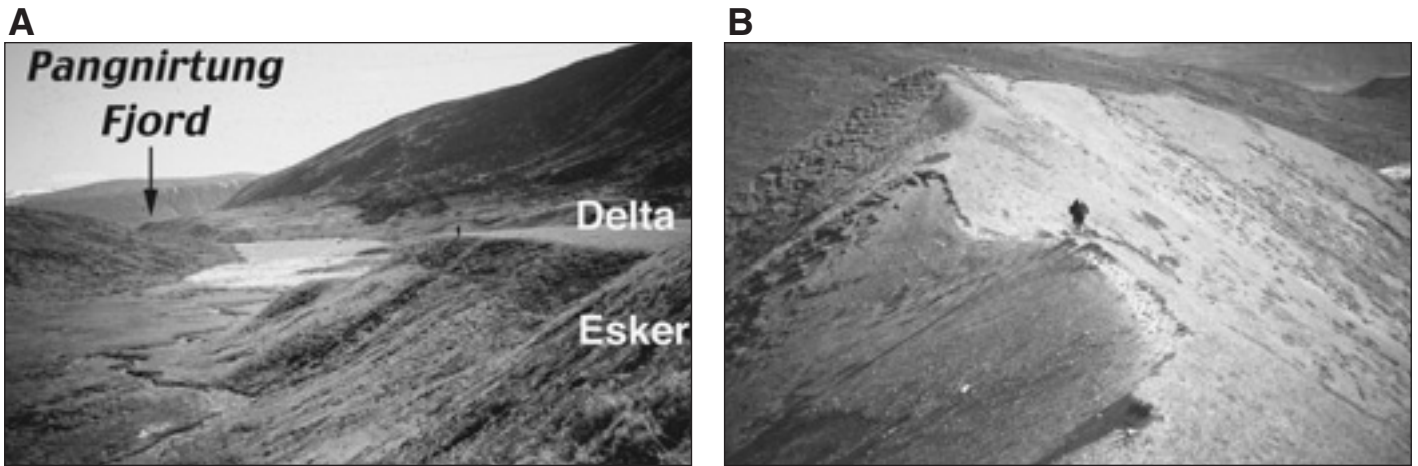


Figure 18. Looking south, toward Pagnirtung Fjord, at (A) the ice-contact delta (1.8 m person on delta surface for scale), and (B) down the surface of the esker in the lower Kolik River valley (1.65 m person for scale; locations shown in Fig. 17).

overriding cold-based ice sheet or local cirque glacier retreated just prior to the main retreat of Penny and/or Laurentide ice in the Kolik River valley and Pagnirtung Fjord.

Our cosmogenic nuclide exposure ages from the Ukalik Lake basin also suggest the presence of glacier ice in the cirque basins during the late Wisconsinan (about 22–11 ka). However, the interpretation is complicated because the single boulder sampled here has an apparent exposure age (22.5 ka) twice that of the striated bedrock samples (11.2 ka), suggesting possible prior exposure of the boulder sample and/or burial, followed by stripping, of the bedrock surface.

In contrast to our cosmogenic data, radiocarbon ages of sediments from Amarak and Ukalik Lakes (Wolfe, 1994, 1996; Wolfe and Härtling, 1996) suggest that both of these basins were last inundated by glacial ice prior to the late Wisconsinan and served as biological refugia. Four accelerator mass spectrometry radiocarbon ages from small samples (<50 mg) of bryophytic moss deposited in silty sediments suggest that mosses were extant on the uplands between 17 and 38 ka (Wolfe, 1996). There is no local source of carbonate in the field area to suggest that the samples have incorporated old carbon; however, it is possible that the mosses were redeposited from older sediments (Wolfe, 1996).

If the 17 and 38 ka radiocarbon ages are taken at face value, then our exposure ages are too young and thus the surfaces we sampled must have either eroded (unlikely as the gneiss is very hard) or been shielded by till, ice, or snow since they were first deglaciated. The older boulder (sample KM95-19; 22.5 ka) overlying the younger bedrock (samples KM95-20 and KM95-21; 11.2 ka) is consistent with a scenario where the bedrock was covered more deeply or for longer than the boulder. However, the boulder must have also been covered for at least some of the time since it was deposited or it would have an exposure age similar to the radiocarbon age of the lake sediments (>38 ka). There was, however, no indication that till or snow had accumulated on the exposed cirque lip from which we collected these samples.

With the few samples we have, we are unable to resolve the discrepancy between the two dating techniques. However, in some places on Baffin Island lake sediments and boulders provide similar ages. For example, Steig et al. (1998) found exposure-dated boulders and radiocarbon-dated lacustrine sediments that provided consistent age limits of ≥ 35 ka for deglaciation of elevations above 450 m on northern Cumberland Peninsula. The disparity between the two dating techniques in our field area needs to be resolved by further sampling and analysis.

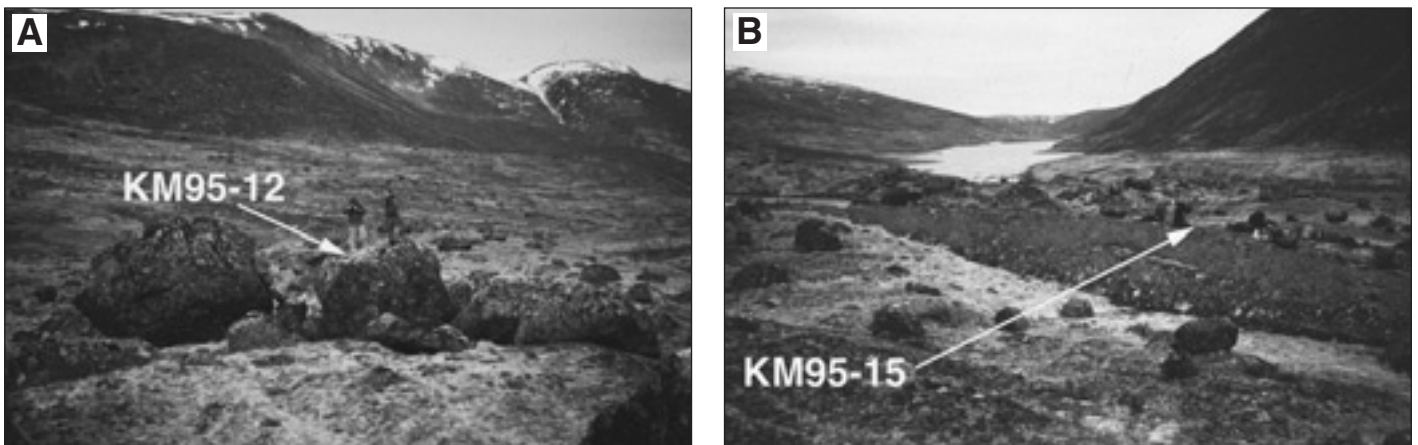


Figure 19. (A) Sample KM95-12, a large erratic boulder (person on right is 1.8 m) and (B) sample KM95-15, from glacially molded bedrock (backpack for scale). Both samples are from the same location in the Kolik River valley bottom; data are summarized in Table 5 (locations shown in Fig. 17).



Figure 20. Looking northeast at Ukalik Lake, showing the steep-walled basin and the location of samples KM95-19 and KM95-20 (1.7 m person for scale); data are summarized in Table 5.

DISCUSSION

Local Implications

Cosmogenic nuclide measurements indicate that late Wisconsinan ice undated Pangnirtung Fjord, adjacent Kingnait Fjord, and the Kolik River valley, in contrast to the existing chronology of the region that suggests these areas were ice free during the late Wisconsinan (Dyke, 1977, 1979; Dyke et al., 1982). Glacier ice filled Pangnirtung Fjord and advanced to the Duval morainal position by about 25 ka. Our cosmogenic exposure ages from the Duval moraines and WZ-2 suggest either continuous ice cover from about 24 to 9 ka or multiple ice-cover events during this same time period. Deglaciation occurred after about 10 ka, resulting in the deposition of a large glaciomarine delta (now raised to 99 m a.s.l.) that formed along Kingnait Fjord as meltwater and sediment drained across the foreland from the Duval morainal position. Following the deposition of this delta, glacial ice appears to have retreated rapidly, producing at least two recessional moraines during withdrawal from Pangnirtung Fjord. Ice filling the Kolik River tributary valley appears to have retreated just prior to ice in Pangnirtung Fjord, between 12 and 11 ka. The chronology of ice retreat in the highlands around Pangnirtung Fjord is less certain; exposure ages and radiocarbon-dated lake sediment suggest different scenarios for ice extent in cirque basins. Exposure ages are consistent with ice filling basins during the late Wisconsinan, whereas radiocarbon ages from lake sediments suggest that these cirques were ice free after 38 ka.

Glacier ice filling Pangnirtung Fjord must represent an expansion of outlet glaciers from the Penny ice cap, which likely merged with expanded Laurentide ice in Foxe basin and adjacent Cumberland Sound. Our data are consistent with previous work suggesting that glacial ice advanced to the outer shelf of Cumberland Sound during the late Wisconsinan and had retreated up the sound by about 10 200 ^{14}C yr B.P. (Jennings et al., 1996). Ice retreat from Cumberland Sound probably initiated the rapid retreat of ice in Pangnirtung and Kingnait Fjords by causing rapid drawdown and calving at the fjord mouths. Cosmogenic nuclide data not reported here (Davis et al., 1996; Marsella, 1998) suggest that Pangnirtung Fjord and Pangnirtung Pass (Fig. 1) were completely deglaciated by about 7.5 ka.

Regional Implications

Our data have significant regional implications and are consistent with other recent studies suggesting that late Wisconsinan glacial ice in the east-

ern Canadian Arctic was far more extensive than previously believed. On northern Cumberland Peninsula, late Wisconsinan ice occupied a fjord below 260 m a.s.l. (Steig et al., 1998). On Ellesmere Island, Devon Island, and in the strait between Ellesmere and Greenland, radiocarbon and exposure ages (Dyke, 1998, 1999; Zreda et al., 1999; England, 1998, 1999) suggest that the Innuitian ice sheet was more extensive during the LGM than previously believed (e.g., England, 1978, 1987, 1996), supporting the work of Blake (1970, 1975, 1992). In Labrador, a variety of dating techniques (e.g., Clark and Josenhans, 1986; Clark et al., 1989; Brook et al., 1998) suggest that the type-Saglek moraines were formed during the late Wisconsinan, rather than earlier (Ives, 1978). Thus, more and more evidence suggests that the northern margins of North American ice sheets were expanded during the LGM; only McCuaig's (1994) limited ^{10}Be data from northern Baffin Island suggest restricted late Wisconsinan ice flow.

The recognition of ice-rafted debris, known as Heinrich layers (Heinrich, 1988; Bond et al., 1992, 1993) and detrital carbonate layers (Andrews, 1998; Andrews et al., 1998a, 1998b), in sediment cores from the North Atlantic Ocean suggest that climate shifted abruptly on a millennial time scale during the Wisconsinan glaciation, and that these events represent a dynamic link in the atmosphere–ice sheet–ocean system (Bond et al., 1993; Broecker, 1994). Determination of provenance of Heinrich and detrital carbonate layers (Dowdeswell et al., 1995; Andrews, 1998; Barber et al., 1998; Hemming et al., 1998) may help resolve whether millennial-scale climate cycles in the Northern Hemisphere are driven by internal ice sheet factors (MacAyeal, 1993) as opposed to external forcing, such as global cooling that causes concomitant alpine glacial advances in the Chilean Andes (Lowell et al., 1995). For example, Andrews et al. (1998b) correlated detrital carbonate events recognized in marine sediment cores from the continental slope of southeast Baffin Island with H-1, H-2, and H-4 in the North Atlantic Ocean. Moreover, Andrews et al. (1998b) identified a black sedimentary unit, lithofacies C, in many sediment cores that could only be derived by glacial erosion of the floor of Cumberland Sound. In North Atlantic sediment cores collected hundreds of kilometers from Baffin Island, Hemming et al. (1998) used stable heavy isotope signatures to suggest that Heinrich layers 2, 4, and 5 must be derived from Precambrian Churchill Province shield rock. Given that this bedrock type underlies most of the Hudson Bay region, including the large fjords along the eastern coast of Baffin Island, it is important to determine whether ice margins extended beyond the heads of these fjords during the late Wisconsinan. Our data suggest additional source regions (to the probable Hudson Strait and Cumberland Sound ice streams) for Heinrich layers.

Lateral and vertical ice extent, hence ice sheet volume, is an important boundary condition for modeling paleoclimate (e.g., Denton and Hughes, 1981; Mix and Ruddiman, 1984; Shackleton, 1987; Tushingham, 1991; Tushingham and Peltier, 1991; Peltier, 1994; Berger et al., 1999). Global sea-level lowering may be the best constraint for estimating ice sheet volume (Kutzbach and Ruddiman, 1993), with 121 ± 5 m being one accepted value for sea-level lowering at 17 000 ^{14}C yr B.P. (Fairbanks, 1989). Many recent studies have suggested that some ice sheet lobes maintained gentler profiles, thus lower ice sheet volume, during the LGM than previously believed (Clark, 1992). Our results indicating a greater late Wisconsinan ice extent in the Pangnirtung and Kingnait Fjord area do not have a great impact on calculations of global ice volume and sea level. For example, even a low-gradient ice lobe filling Cumberland Sound (Jennings, 1993; Jennings et al., 1996; Kaplan et al., 1998, 1999) would provide a greater ice volume than filling Pangnirtung and Kingnait Fjords. But, if glacial ice filled the tens to hundreds of other fjords in the eastern Canadian Arctic during the LGM, then the total ice volume would increase, especially if high-altitude accumulation zones for respective outlet glaciers are also considered. Moreover, these ice streams could have fed extensive ice shelves during the late Wisconsinan, as proposed by Denton and Hughes (1981).

CONCLUSIONS

This study substantially revises the glacial chronology of the Pangnirtung Fjord area and demonstrates the utility of cosmogenic exposure dating for distinguishing ages of Arctic glacial landscapes. Our five most important conclusions are the following.

1. Pangnirtung and Kingnait Fjords were ice filled during the late Wisconsinan rather than ice free, as suggested by earlier mapping.
2. The prominent Duval moraines are at least 35 k.y. younger than previously believed and do not mark the boundary between weathering zones of different ages.
3. Some of our late Wisconsinan ages for cirque glaciation are in conflict with radiocarbon data from lake sediments that suggest less extensive late Wisconsinan ice.
4. Our data are in agreement with marine-based evidence from nearby Cumberland Sound, which taken together contrast the restricted Laurentide ice sheet paradigm.
5. Our data suggest that the northern and southern margins of the Laurentide ice sheet were generally in phase during the Wisconsinan glaciation.

ACKNOWLEDGMENTS

We thank P. Hackett, C. Killian, J. Leonard, C. Massey, J. Turner, and the staff of Parks Canada for field assistance, J. Southon and R. Finkel at Lawrence Livermore National Laboratory (LLNL) Center for Accelerator Mass Spectrometry for analytical assistance, J. Stone and one anonymous reader for formal reviews, and P. Clark, J. Andrews, and M. Kaplan for helpful comments on the manuscript. This project was funded by the National Science Foundation grant OPP-93-21733, with additional support from the American Association of Petroleum Geologists and Bentley College. LLNL work is supported by U.S. Department of Energy contract W-7405-ENG-48.

REFERENCES CITED

- Aksu, A.E., and Mudie, P.J., 1985, Late Quaternary stratigraphy and paleoecology of northwest Labrador Sea: *Marine Micropaleontology*, v. 9, p. 537–557.
- Andrews, J.T., 1975, Support for a stable late Wisconsin ice margin (14,000 to ca. 9,000 BP); a test based on glacial rebound: *Geology*, v. 3, p. 617–620.
- Andrews, J.T., 1987, The Late Wisconsin glaciation and deglaciation of the Laurentide Ice Sheet, in Ruddiman, W.F., and Wright, H.E., Jr., eds., *North America and adjacent oceans during the last deglaciation*: Boulder, Colorado, Geological Society of America, *Geology of North America*, v. K-3, p. 13–37.
- Andrews, J.T., 1998, Abrupt changes (Heinrich events) in late Quaternary North Atlantic marine environments: A history and review of data and concepts: *Journal of Quaternary Science*, v. 13, p. 3–16.
- Andrews, J.T., and Ives, J.D., 1978, “Cockburn” nomenclature and the late Quaternary history of the eastern Canadian Arctic: *Arctic and Alpine Research*, v. 10, p. 617–633.
- Andrews, J.T., Szabo, B.J., and Isherwood, W., 1975, Multiple tills, radiometric ages, and assessment of the Wisconsin glaciation in eastern Baffin Island: *Arctic and Alpine Research*, v. 7, p. 39–60.
- Andrews, J.T., Kirby, M.E., Aksu, A., Barber, D.C., and Meese, D., 1998a, Late Quaternary detrital carbonate (DC-) layers in Baffin Bay marine sediments (67°–74°N): Correlation with Heinrich events in the North Atlantic?: *Quaternary Science Reviews*, v. 17, p. 1125–1137.
- Andrews, J.T., Kirby, M., Jennings, A.E., and Barber, D.C., 1998b, Late Quaternary stratigraphy, chronology, and depositional history on the slope of S.E. Baffin Island, detrital carbonate and Heinrich events: Implications for onshore glacial history: *Géographie Physique et Quaternaire*, v. 52, p. 91–105.
- Barber, D.C., Andrews, J.T., Farmer, G.L., Jennings, A.E., and Kaplan, M.R., 1998, Constraints on Laurentide ice stream dynamics from sediment provenance studies in Hudson Strait and the Labrador Sea: *Geological Society of America Abstracts with Programs*, v. 30, no. 7, p. A51.
- Berger, A., Li, X.S., and Loutre, M.F., 1999, Modelling Northern Hemisphere ice volume over the last 3 Ma: *Quaternary Science Reviews*, v. 18, p. 1–11.
- Bierman, P.R., Marsella, K.A., Patterson, C., Davis, P.T., and Caffee, M., 1999, Mid-Pleistocene cosmogenic minimum-age limits for pre-Wisconsinan glacial surfaces in southwestern Minnesota and southern Baffin Island: A multiple nuclide approach: *Geomorphology*, v. 27, p. 25–39.
- Birkeland, P.W., 1978, Soil development as an indication of relative age of Quaternary deposits, Baffin Island, N.W.T., Canada: *Arctic and Alpine Research*, v. 10, p. 733–747.
- Blake, W., Jr., 1970, Studies of glacial history in Arctic Canada, I. Pumice, radiocarbon dates, and differentiated postglacial uplift in the eastern Queen Elizabeth Islands: *Canadian Journal of Earth Sciences*, v. 7, p. 634–664.
- Blake, W., Jr., 1975, Radiocarbon age determinations and postglacial emergence at Cape Storm, southern Ellesmere Island, Arctic Canada: *Geografiska Annaler*, v. A57, p. 1–71.
- Blake, W., Jr., 1992, Holocene emergence at Cape Herschel, east-central Ellesmere Island, Arctic Canada: Implications for ice sheet configuration: *Canadian Journal of Earth Sciences*, v. 29, p. 1958–1980.
- Bockheim, J.G., 1979, Properties and relative ages of soils of southwestern Cumberland Peninsula, Baffin Island, N.W.T., Canada: *Arctic and Alpine Research*, v. 11, p. 289–304.
- Bond, G., Heinrich, H., Broecker, W., Labeyrie, L., McManus, J., Andrews, J., Houn, S., Jantschik, R., Clasen, S., Simet, C., Tedesco, K., Klas, M., Bonani, G., and Ivy, S., 1992, Evidence for massive discharges of icebergs into the North Atlantic ocean during the last glacial period: *Nature*, v. 360, p. 245–249.
- Bond, G., Broecker, W.S., Johnsen, S., McManus, J., Labeyrie, L., Jouzel, J., and Bonani, G., 1993, Correlations between climate records from North Atlantic sediments and Greenland ice: *Nature*, v. 365, p. 143–147.
- Boyer, S.J., and Pheasant, D.R., 1974, Delimitation of weathering zones in the fjord area of eastern Baffin Island, Canada: *Geological Society of America Bulletin*, v. 85, p. 805–810.
- Broecker, W.S., 1994, Massive iceberg discharges as triggers for global climate change: *Nature*, v. 372, p. 421–424.
- Brook, E.J., Kurz, M.D., Denton, G.H., and Ackert, R.P.J., 1993, Chronology of Taylor Glacier advances in Arena Valley, Antarctica using in situ cosmogenic ³He and ¹⁰Be: *Quaternary Research*, v. 39, p. 11–23.
- Brook, E., Clark, P., Lehman, S., Nesje, A., Raisbeck, G., and Yiou, F., 1998, ¹⁰Be chronology of weathering zones in Norway and Labrador: *Geological Society of America Abstracts with Programs*, v. 30, no. 7, p. A300.
- Brown, E.T., Edmond, J.M., Raisbeck, G.M., Yiou, F., Kurz, M.D., and Brook, E.J., 1991, Examination of surface exposure ages of Antarctic moraines using in situ produced ¹⁰Be and ²⁶Al: *Geochimica et Cosmochimica Acta*, v. 55, p. 2269–2283.
- Clark, D.H., Bierman, P.R., and Larsen, P., 1995, Improving in situ cosmogenic chronometers: *Quaternary Research*, v. 44, p. 367–377.
- Clark, P.U., 1992, Surface form of the southern Laurentide Ice Sheet and its implications to ice-sheet dynamics: *Geological Society of America Bulletin*, v. 104, p. 595–605.
- Clark, P.U., and Josenhans, H.W., 1986, Late Quaternary land-sea correlations, northern Labrador and Labrador Shelf, in *Current research, Part B: Geological Survey of Canada Paper 86-1B*, p. 171–178.
- Clark, P.U., Short, S.K., Williams, K.M., and Andrews, J.T., 1989, Late Quaternary chronology and environments of Square Lake, Torngat Mountains, Labrador: *Canadian Journal of Earth Sciences*, v. 26, p. 2130–2144.
- Coleman, A.P., 1920, Extent and thickness of the Labrador Ice Sheet: *Geological Society of America Bulletin*, v. 31, p. 319–328.
- Daly, R.A., 1902, The geology of the northeast coast of Labrador: *Harvard University Museum of Comparative Zoology Bulletin*, v. 66, p. 1499–1520.
- Davis, P.T., 1988, Possible evidence for extensive late Wisconsin (late Foxe) glaciation in Pangnirtung Pass area, southern Cumberland Peninsula, Baffin Island: *Geological Society of America Abstracts with Programs*, v. 20, no. 7, p. 208.
- Davis, P.T., Finkel, R.C., Caffee, M.W., Southon, J.R., and Koning, J., 1992, Cosmogenic ²⁶Al and ¹⁰Be exposure ages for glacially eroded bedrock, Pangnirtung area, Baffin Island, Canada: *Geological Society of America Abstracts with Programs*, v. 24, no. 6, p. A-461.
- Davis, P.T., Marsella, K.A., Bierman, P.R., and Caffee, M.W., 1996, Paired glacial boulders and bedrock cosmogenic analyses: *Eos (Transactions, American Geophysical Union)*, v. 77, p. F193.
- Davis, P.T., Bierman, P.R., Marsella, K.A., Caffee, M.W., and Southon, J.R., 1999, Cosmogenic analysis of glacial terrains in the eastern Canadian Arctic: A test for inherited nuclides and the effectiveness of glacial erosion: *Annals of Glaciology* (in press), v. 28, p. 181–188.
- Denton, G.H., and Hughes, T.J., 1981, *The last great ice sheets*: New York, Wiley-Interscience, 484 p.
- Dowdeswell, J.A., Maslin, M.A., Andrews, J.T., and McCave, I.N., 1995, Iceberg production, debris rafting, and the extent and thickness of Heinrich layers (H-1, H-2) in North Atlantic sediments: *Geology*, v. 23, p. 301–304.
- Dyke, A.S., 1977, Quaternary geomorphology, glacial chronology, and climatic and sea-level history of southwestern Cumberland Peninsula, Baffin Island, Northwest Territories, Canada [Ph.D. dissert.]: Boulder, University of Colorado, 184 p.
- Dyke, A.S., 1979, Glacial and sea-level history of southwestern Cumberland Peninsula, Baffin Island, N.W.T., Canada: *Arctic and Alpine Research*, v. 11, p. 179–202.
- Dyke, A.S., 1998, Holocene deleveling of Devon Island, Arctic Canada: Implications for ice sheet geometry and crustal response: *Canadian Journal of Earth Sciences*, v. 35, p. 885–904.
- Dyke, A.S., 1999, Last Glacial Maximum and deglaciation of Devon Island, Arctic Canada: Support for an Inuitian ice sheet: *Quaternary Science Reviews*, v. 18, p. 393–420.
- Dyke, A.S., and Prest, V.K., 1987, The late Wisconsinan and Holocene history of the Laurentide Ice Sheet: *Géographie Physique et Quaternaire*, v. 41, p. 237–263.
- Dyke, A.S., Andrews, J.T., and Miller, G.H., 1982, Quaternary geology of the Cumberland Peninsula, Baffin Island, District of Franklin: *Geological Survey of Canada Memoir 403*, 2 maps, 32 p.
- England, J., 1978, The glacial geology of northeastern Ellesmere Island, Northwest Territories, Canada: *Canadian Journal of Earth Sciences*, v. 15, p. 603–617.
- England, J., 1987, Glaciation and the evolution of the Canadian High Arctic landscape: *Geology*, v. 15, p. 419–424.
- England, J., 1996, Glacier dynamics and paleoclimatic change during the last glaciation of eastern Ellesmere Island, Canada: *Canadian Journal of Earth Sciences*, v. 33, p. 779–799.
- England, J., 1998, Support for the Inuitian Ice Sheet in the Canadian High Arctic during the Last Glacial Maximum: *Journal of Quaternary Science*, v. 13, p. 275–280.

- England, J., 1999, Coalescent Greenland and Inuitian ice during the Last Glacial Maximum: Revisiting the Quaternary of the Canadian High Arctic: *Quaternary Science Reviews*, v. 18, p. 421–456.
- Fairbanks, R.G., 1989, A 17,000-year glacio-eustatic sea level record: influence of glacial melting rates on the Younger Dryas event and deep-ocean circulation: *Nature*, v. 342, p. 637–642.
- Fisher, D.A., Koerner, R.M., Bourgeois, J.C., Zielinski, G., Wake, C., Hammer, C.U., Clausen, H.B., Gundestrup, N., Johnsen, S., Goto-Azuma, K., Hondoh, T., Blake, E., and Gerasimoff, M., 1998, Penny Ice Cap cores, Baffin Island, Canada, and the Wisconsin Foxe dome connection: Two states of Hudson Bay ice cover: *Science*, v. 279, p. 692–695.
- Flint, R.F., 1943, Growth of the North American ice sheet during the Wisconsin Age: *Geological Society of America Bulletin*, v. 54, p. 325–362.
- Gilbert, R., and Church, M., 1983, Contemporary sedimentary environments of Baffin Island, N.W.T., Canada: Reconnaissance of lakes on Cumberland Peninsula: *Arctic and Alpine Research*, v. 15, no. 3, p. 321–332.
- Gosse, J.C., Klein, J., Evenson, E.B., Lawn, B., and Middleton, R., 1995, Beryllium-10 dating of the duration and retreat of the last Pinedale glacial sequence: *Science*, v. 268, p. 1329–1333.
- Grosswald, M.G., 1984, Glaciation of the continental shelf (Part I): *Polar Geography and Geology*, v. 8, p. 196–258.
- Hallet, B., and Putkonen, J., 1994, Surface dating of dynamic landforms: Young boulders on aging moraines: *Science*, v. 265, p. 937–940.
- Heinrich, H., 1988, Origin and consequences of cyclic ice rafting in the Northeast Atlantic Ocean during the past 13,000 years: *Quaternary Research*, v. 29, p. 143–152.
- Hemming, S.R., Broecker, W.S., Sharp, W.D., Bond, G.C., Gwiazda, R.H., McManus, J.F., Klas, M., and Hajdas, I., 1998, Provenance of Heinrich layers in core V28-82, northeastern Atlantic: $^{40}\text{Ar}/^{39}\text{Ar}$ ages of ice-rafted hornblende, Pb isotopes in feldspar grains, and Nd-Sr-Pb isotopes in the fine fraction: *Earth and Planetary Science Letters*, v. 164, p. 317–333.
- Hughes, T.J., 1987, Ice dynamics and deglaciation models when ice sheets collapsed, *in* Ruddiman, W.F., and Wright, H.E., Jr., eds., *North America and adjacent oceans during the last deglaciation*: Boulder, Colorado, Geological Society of America, *Geology of North America*, v. K-3, p. 183–220.
- Hughes, T.J., Denton, G.H., and Grosswald, M.G., 1977, Was there a late Würm Arctic ice sheet?: *Nature*, v. 266, p. 596–602.
- Ives, J.D., 1978, The maximum extent of the Laurentide Ice Sheet along the east coast of North America during the last deglaciation: *Arctic*, v. 32, p. 24–35.
- Jackson, G.D., and Taylor, F.C., 1972, Correlation of major Aphebian rock units in the northern Canadian Shield: *Canadian Journal of Earth Sciences*, v. 9, p. 1650–1669.
- Jennings, A.E., 1989, The Quaternary history of Cumberland Sound, Baffin Island, Arctic Canada [Ph.D. dissert.]: Boulder, University of Colorado, 319 p.
- Jennings, A.E., 1993, The Quaternary history of Cumberland Sound, southeastern Baffin Island: The marine evidence: *Géographie Physique et Quaternaire*, v. 47, p. 21–42.
- Jennings, A.E., Tedesco, K.A., Andrews, J.T., and Kirby, M.E., 1996, Shelf erosion and glacial proximity in the Labrador Sea during and after Heinrich events (H-3 or 4 to H-0) as shown by foraminifera, *in* Andrews, J.T., Austin, W.E.N., Bergsten, H., and Jennings, A.E., eds., *Late Quaternary paleoceanography of the North Atlantic margins*: London, Geological Society Special Publications 111, p. 29–49.
- Kaplan, M.R., Steig, E.J., and Miller, G.H., 1998, A new model of the late Quaternary Laurentide Ice Sheet and local glaciation in the Cumberland Sound region, eastern Canadian Arctic: *Geological Society of America Abstracts with Programs*, v. 30, no. 7, p. A111.
- Kaplan, M.R., Pfeffer, W.T., Sassolas, C., and Miller, G.H., 1999, Numerical modelling of the Laurentide Ice Sheet in the Baffin Island region: The role of a Cumberland Sound ice stream: *Canadian Journal of Earth Sciences*, v. 36, no. 8, p. 1315–1326.
- Kohl, C.P., and Nishiizumi, K., 1992, Chemical isolation of quartz for measurement of in situ produced cosmogenic nuclides: *Geochimica et Cosmochimica Acta*, v. 56, p. 3583–3587.
- Kutzbach, J.E., and Ruddiman, W.F., 1993, Model description, external forcing, and surface boundary conditions, *in* Wright, H.E., Jr., et al., eds., *Global climates since the Last Glacial Maximum*: Minneapolis, University of Minnesota Press, p. 12–23.
- Lal, D., 1991, Cosmic ray labeling of erosion surfaces: In situ production rates and erosion models: *Earth and Planetary Science Letters*, v. 104, p. 424–439.
- Larsen, P.L., 1996, In-situ production rates of cosmogenic ^{10}Be and ^{26}Al over the past 21,500 years determined from the terminal moraine of the Laurentide Ice Sheet, north-central New Jersey [Master's thesis]: Burlington, University of Vermont, 129 p.
- Lemmen, D.S., Gilbert, R., Smol, J., and Hall, R., 1988, Holocene sedimentation in glacial Tasikutaq Lake, Baffin Island: *Canadian Journal of Earth Sciences*, v. 25, p. 810–823.
- Locke, W.W., III, 1979, Etching of hornblende grains in Arctic soils: An indicator of relative age and paleoclimate: *Quaternary Research*, v. 11, p. 197–212.
- Løken, O.H., 1966, Baffin Island refugia older than 54,000 years: *Science*, v. 153, p. 1378–1380.
- Lowell, T.V., Heusser, C.J., Anderson, B.G., Moreno, P.I., Hauser, A., Heusser, L.E., Schluchter, C., Marchant, D.R., and Denton, G.H., 1995, Interhemispheric correlation of late Pleistocene glacial events: *Science*, v. 269, p. 1541–1549.
- MacAyeal, D.R., 1993, Binge/purge oscillations of the Laurentide ice sheet as a cause of the northern Atlantic's Heinrich events: *Paleoceanography*, v. 8, p. 775–784.
- Marsella, K.A., 1998, Timing and extent of glaciation in the Pangnirtung Fjord region, southern Cumberland Peninsula: Determined using in situ produced cosmogenic ^{10}Be and ^{26}Al [Master's thesis]: Burlington, University of Vermont, 135 p.
- Marsella, K.A., Davis, P.T., Bierman, P.R., Finkel, R.C., Caffee, M.W., and Southon, J.R., 1995, Geologic test of the weathering zone concept and nunatak hypothesis using cosmogenic isotope dating in the Pangnirtung Fjord area, Baffin Island, Nunavut Territory, Canada: *Geological Society of America Abstracts with Programs*, v. 27, no. 6, p. A59.
- Maxwell, J.B., 1980, The climate of the Canadian Arctic Islands and adjacent waters: Ottawa, Canadian Government Publishing Centre, 71 p.
- Mayewski, P.M., Denton, G.H., and Hughes, T.J., 1981, Late Wisconsin ice sheets in North America, *in* Denton, G.H., and Hughes, T.J., eds., *The last great ice sheets*: New York, John Wiley & Sons, p. 67–178.
- McCuagig, S.J., 1994, Glacial chronology of the south Bylot and Salmon River lowlands, N.W.T., using erratic dispersal patterns, cosmogenic dating, radiocarbon dating and lichenometry [Master's thesis]: Ottawa, Canada, Carleton University, 140 p.
- Miller, G.H., 1973, Late-Quaternary glacial and climatic history of northern Cumberland Peninsula, Baffin Island, N.W.T., Canada: *Quaternary Research*, v. 3, p. 561–583.
- Miller, G.H., and Dyke, A.S., 1974, Proposed extent of late Wisconsin Laurentide ice on Baffin Island: *Geology*, v. 2, p. 125–130.
- Miller, G.H., Andrews, J.T., and Short, S.K., 1977, The last interglacial-glacial cycle, Clyde foreland, Baffin Island, N.W.T.: Stratigraphy, biostratigraphy, and chronology: *Canadian Journal of Earth Sciences*, v. 14, p. 2824–2857.
- Mix, A.C., and Ruddiman, W.F., 1984, Oxygen-isotope analyses and Pleistocene ice volumes: *Quaternary Research*, v. 21, p. 1–20.
- Nelson, A.R., 1980, Chronology of Quaternary landforms, Qivitu Peninsula, northern Cumberland Peninsula, Baffin Island, N.W.T., Canada: *Arctic and Alpine Research*, v. 12, p. 265–286.
- Nishiizumi, K., Winterer, E.L., Kohl, C.P., Klein, J., Middleton, R., Lal, D., and Arnold, J.R., 1989, Cosmic ray production rates of ^{10}Be and ^{26}Al in quartz from glacially polished rocks: *Journal of Geophysical Research*, v. 94, p. 17907–17915.
- Odell, N.E., 1933, The mountains of northern Labrador: *Geographical Journal*, v. 82, p. 193–210.
- Peltier, W.R., 1994, Ice age paleotopography: *Science*, v. 265, p. 195–201.
- Pheasant, D.R., and Andrews, J.T., 1973, Wisconsin glacial chronology and relative sea level movements, Narpaing Fjord/Broughton Island area, eastern Baffin Island: *Canadian Journal of Earth Sciences*, v. 10, p. 1621–1641.
- Shackleton, N.J., 1987, Oxygen isotopes, ice volume and sea level: *Quaternary Science Reviews*, v. 6, p. 183–190.
- Steig, E.J., Wolfe, A.P., and Miller, G.H., 1998, Wisconsinan refugia and the glacial history of eastern Baffin Island, Arctic Canada: Coupled evidence from cosmogenic isotopes and lake sediments: *Geology*, v. 26, p. 835–838.
- Stuiver, M., and Reimer, P.J., 1993, Radiocarbon calibration program Rev. 3.0.3A-Mac test Version #6: *Radiocarbon*, v. 35, p. 215–230.
- Sugden, D.E., 1977, Reconstruction of the morphology, dynamics, and thermal characteristics of the Laurentide Ice Sheet: *Arctic and Alpine Research*, v. 9, p. 21–47.
- Sugden, D.E., and Watts, S.H., 1977, Tors, felsenmeer, and glaciation in northern Cumberland Peninsula, Baffin Island: *Canadian Journal of Earth Sciences*, v. 14, p. 2817–2823.
- Tushingham, A.M., 1991, On the extent and thickness of the Inuitian Ice Sheet: A postglacial adjustment approach: *Canadian Journal of Earth Sciences*, v. 28, p. 231–238.
- Tushingham, A.M., and Peltier, W.R., 1991, ICE-3G: A new global model of late Pleistocene deglaciation based upon geophysical predictions of postglacial relative sea level change: *Journal of Geophysical Research*, v. 96B, p. 4497–4523.
- Wolfe, A.P., 1994, Late Wisconsinan and Holocene diatom stratigraphy from Amarak Lake, Baffin Island, N.W.T., Canada: *Journal of Paleolimnology*, v. 10, p. 129–139.
- Wolfe, A.P., 1996, Wisconsinan refugial landscapes, eastern Baffin Island, Northwest Territories: *The Canadian Geographer*, v. 40, p. 81–87.
- Wolfe, A.P., and Hartling, J.W., 1996, The late Quaternary development of three ancient tarns on southwestern Cumberland Peninsula, Baffin Island, Arctic Canada: paleolimnological evidence from diatoms and sedimentary chemistry: *Journal of Paleolimnology*, v. 15, p. 1–18.
- Zreda, M., England, J., Phillips, F., Elmore, D., and Sharma, P., 1999, Unblocking of the Nares Strait by Greenland and Ellesmere ice-sheet retreat 10,000 years ago: *Nature*, v. 398, p. 139–142.

MANUSCRIPT RECEIVED BY THE SOCIETY MAY 14, 1999

REVISED MANUSCRIPT RECEIVED JULY 23, 1999

MANUSCRIPT ACCEPTED SEPTEMBER 16, 1999